A METHOD FOR EXPERIMENTALLY DETERMINING ROTATIONAL MOBILITIES

by

STANLEY SIMON SATTINGER

B.M.E., Georgia Institute of Technology
(1962)

M.S., Cornell Univeristy
(1964)

SUBMITTED IN PARTIAL FULFILLMENT
OF THE REQUIREMENTS FOR THE
DEGREE OF

MASTER OF SCIENCE

at the

MASSACHUSETTS INSTITUTE OF TECHNOLOGY

August, 1978

Signature redacted

Signature of Author..
Department of Mechanical Engineering, August 11, 1978

Signature redacted

Certified By..............................
Thesis Supervisor

Signature redacted

Accepted By...
Chairman, Department Committee on Graduate Students

A METHOD FOR EXPERIMENTALLY DETERMINING ROTATIONAL MOBILITIES

by

Stanley Simon Sattinger

Submitted to the Department of Mechanical Engineering on August 11, 1978 in partial fulfillment of the requirements for the Degree of Master of Science.

ABSTRACT

Mobility functions involving rotational velocities and moment excitations must be determined for the prediction of the responses of certain types of structures in dynamic analyses. Previous investigators have approached the difficult task of experimentally measuring such mobilities with the use of special fixturing attached to the structures. It is shown that rotational mobilities of structures are equivalent to spatial derivatives of their translational mobilities. The method of finite differences is adapted to the approximation of these derivatives. By this approach the rotational mobilities are derived from sets of conventionally measured translational mobilities, eliminating the need for special fixturing.

This method of determining rotational mobilities is demonstrated in a set of experiments on a free-free beam. Good agreement is obtained between experimentally and theoretically generated versions of two rotational velocity/force mobilities. An experimentally derived rotational velocity/moment mobility is found to

give reasonably good indications of resonances, but exhibits large amounts of scatter in some frequency bands. This scatter is attributed to the subtraction of translational mobility quantities which are nearly equal in magnitude with resultant magnification of minor irregularities present in them. Further investigation is recommended to determine an effective method of smoothing the translational mobility data before the differencing calculations to eliminate this scatter.

The finite difference method of determining rotational mobilities is seen to accommodate considerable variation in the spacings of the points where the constituent translational mobilities are measured.

Thesis Supervisor: Richard H. Lyon

Title: Professor, Department of Mechanical Engineering

ACKNOWLEDGEMENTS

I wish to thank Professor Richard H. Lyon for his guidance and suggestions and for his willingness to support me in an area of study which was of a great deal of personal interest to me.

I am also grateful to Professor Emmett A. Witmer of the Department of Aeronautics and Astronautics for his aid in connection with the method of finite differences. Many thanks go to fellow student Charles Gedney for his pointers on the operation of the Acoustics and Vibration Laboratory minicomputer; to Dr. Richard DeJong of Cambridge Collaborative, Inc. for sharing some of his vibration testing experience; and to Mary Toscano for her diligence in the typing of this thesis.

I owe a debt of gratitude to my employer, Westinghouse Electric Corporation, for having awarded me a B.G. Lamme Graduate Scholarship enabling me to pursue a course of study in vibration and acoustics at MIT.

I am especially thankful to my wife, Jerry, and to our daughters, Julia and Allison, for the encouragement they gave me and the many hours of family time they sacrificed throughout the year of my studies at MIT.

TABLE OF CONTENTS

TABLE OF CONTENTS (CONTINUED)

LIST OF FIGURES

LIST OF FIGURES (CONTINUED)

LIST OF FIGURES (CONTINUED)

NOMENCLATURE

A	Uniform beam cross-section area; also the complex amplitude of acceleration
C_i	Constant coefficient of the ith term in the expression for $W(x)$
D_r	Arbitrary multiplier of the rth eigenfunction of a free vibration problem
E	Modulus of elasticity of beam material
e	Base of natural logarithms
$\left.\begin{matrix} F(\omega;\xi) \\ F(\omega) \end{matrix}\right\}$	Complex amplitude of sinusoidally varying force applied at position ξ on a structure.
$F_A(\omega)$	Complex amplitude of the sinusoidally varying force $f_A(t)$
f	Cyclic frequency, Hz
$f_A(t)$	Concentrated force applied at Point A on a structure
$f(x,t)$	Distributed loading applied to a beam, including damping forces
$f_a(x,t)$	Distributed loading applied to beam, exclusive of damping forces
G_{AF}	Cross spectral density of stationary random acceleration and random force (complex function of cyclic frequency)
G_{FF}	Power spectral density of stationary random force (real function of cyclic frequency)
I	Uniform beam cross-section area moment of inertia
i	$\sqrt{-1}$
ℓ	Length of beam
$M(\omega)$	Complex amplitude of sinusoidally varying moment applied at position ξ on a structure

$M_A(\omega)$	Complex amplitude of the sinusoidally varying moment $m_A(t)$
M_r	Modal mass of the rth mode of vibration
m	Total mass of beam
$m_A(t)$	Concentrated moment applied at Point A on a structure
N	Mode number at which infinite series of modal mobilities is truncated
$P(\omega)$	Complex amplitude of the sinusoidally varying force $p(t)$
$p(t)$	One member of a force couple equivalent to moment $m_A(t)$
p_r	The rth eigenvalue of a free vibration problem
$Q_r(t)$	Modal force of the rth mode of vibration
$Q_{ra}(t)$	Modal force of the rth mode exclusive of damping forces
$q_r(t)$	Generalized coordinate or generalized displacement of the rth mode of vibration
t	Time
$W(x)$	Complex amplitude of the sinusoidally varying displacement $w(x,t)$
$W_r(x)$	The rth eigenfunction of a free vibration problem
$\left.\begin{matrix}\dot{W}(\omega;\eta)\\ \dot{W}(\omega)\end{matrix}\right\}$	Complex amplitude of sinusoidally varying translational velocity measured at position η on a structure
$\dot{W}_A(\omega)$	Complex amplitude of sinusoidally varying translational velocity measured at Point A on a structure

NOMENCLATURE (Continued)

$w(x,t)$	Transverse displacement at location x on a beam
$w_A(t)$	Displacement measured at Point A on a structure
$X_r(\omega)$	Complex amplitude of the sinusoidally varying generalized displacement $q_r(t)$
x	Coordinate of axial position on a structure
$Y_{W_A F_B}(\omega)$	Translational velocity/force mobility: velocity measured at A, excitation applied at B
$Y_{W_A M_B}(\omega)$	Translational velocity/moment mobility: velocity measured at A, excitation applied at B
$Y_{\theta_A F_B}(\omega)$	Rotational velocity/force mobility: velocity measured at A, excitation applied at B
$Y_{\theta_A M_B}(\omega)$	Rotational velocity/moment mobility: velocity measured at A, excitation applied at B
z	Coordinate of transverse position on a structure
$\delta(x)$	Dirac delta function of position coordinate x
ϵ	Spacing of the members p(t) of a force couple
ζ_r	Equivalent viscous damping ratio of the rth mode of vibration
η	Axial coordinate of point of velocity measurement on a structure
$\Delta\eta$	Spacing between adjacent velocity measurement locations
$\left.\begin{matrix}\dot{\Theta}(\omega,\eta)\\ \dot{\Theta}(\omega)\end{matrix}\right\}$	Complex amplitude of sinusoidally varying rotational velocity measured at position η on a structure
$\dot{\Theta}_A(\omega)$	Complex amplitude of sinusoidally varying rotational velocity at Point A on a structure
$\theta_A(t)$	Rotation occurring at Point A on a structure
ξ	Axial coordinate of point of excitation on a structure

NOMENCLATURE (Continued)

$\Delta \xi$	Spacing between adjacent excitation points on a structure
ρ	Mass density of beam material
ϕ	Mobility phase angle
ϕ_{AF}	Acceleration/force cross spectral density phase angle (function of cyclic frequency)
$\phi_r(x)$	The portion of the rth eigenfunction $W_r(x)$ exclusive of the multipler D_r
$\psi_{m,n}$	One of a set of translational velocity/force mobilities from which one or more rotational motilities will be derived
ω	Angular frequency, rad/sec
ω_M	A particular value of frequency

I. INTRODUCTION

A. Background

The application of mobility functions* and their inverse quantities, mechanical impedances, to practical problems in vibration, shock, and acoustics has been treated extensively in the literature. Mobility and impedance concepts are readily adaptable to dynamic response predictions for assemblages of two or more component structures.

A mobility function is a transfer function relating the complex amplitude of motion at some point on a structure in response to the complex amplitude of an excitation force applied at any point on the same structure. In the most commonly discussed type of mobility the response motion is a translational component of velocity, and the excitation is a translational force as illustrated in the transfer mobility example of Figures 1.1(a). However, the concept of mobility can be extended to rotational velocities and moment excitations as shown in the examples of Figures 1.1(b) through 1.1(d). A matrix relationship involving the transfer mobilities thus defined between the two points is shown in Figure 1.1(e).

The matrix formulation shown in Figure 1.1(e) can be specialized to the case where the response measurement point, B,

*Also denoted as admittances or receptances.

is coincident with the excitation point, A, i.e., each matrix element is a driving point mobility; or it can be generalized to include the existence of motions and excitations at both points. In the latter instance the second order mobility matrix shown would be expanded to the fourth order. Generalizing still further, the transfer mobility matrix shown in Figure 1.1(e) could be extended to the six possible senses of motion and applied excitation in a three-dimensional application, attaining order 6. The mobility matrix would be enlarged still further as additional locations for responses and excitations would be considered.

In many instances the mobility or impedance quantities are determined experimentally. In cases such as the applications of impedance methods to vibration testing described in References (1) and (2), the motions and forces involved are limited to translational effects directed along a single axis. In the studies described in References (3), (4), and (5), the applications are broadened to treat the interconnection of components which may sustain rotational and translational components of motion, but are assumed to have only translational interaction effects. For an assemblage to be accurately modeled by such an approach, there must be negligibly small moment reactions among components at each interface in the actual system by virtue of joint configuration, symmetry, or other factors.

Cantilevered assemblages can be readily conceived wherein the most important interactions are rotational; in such cases there must be compatibility of rotations at connections, and moment reactions are far more significant than force interactions. Extensions of mobility and impedance methods to response predictions in these cases have been hampered by difficulties in experimentally measuring the rotational mobilities. Whereas the measurement of translational velocities and forces is presently a routine process, apparatus for the measurement of rotational velocities and moments in structural dynamics applications is not commercially available. Noiseux and Meyer (6) suggest that the lack of a general measurement technique has retarded the application of mobility concepts and in some cases has distorted the applications by mandating the use of what can be measured rather than what should be measured.

Explorations of methods for the measurement of moment excitations and rotation responses are described in References (7), (8) and (9). In each of these studies a special fixture has been attached to the structure being measured, and conventional linear force gages and accelerometers have been, in turn, mounted at various locations on the fixture. By appropriate algebraic operations on the data gathered in each of the various measurement configurations, rotational mobilities have been obtained with varying degrees of success. Corrections for the dynamic influences of the fixturing have been required in each case.

B. Scope

The objective of this thesis is to improvise and demonstrate a method of generating experimental rotational mobility functions using conventional measurement techniques without a requirement for the use of special fixturing. The approach taken has been to represent mobilities involving rotational velocities and moment excitations as spatial derivatives of conventional translational mobilities; the derivatives are approximated as finite difference sums of sets of these translational mobilities. In Section II, the theoretical basis and calculational methods for these representations are developed. Section III describes the experimental and theoretical determination of mobilities of a free-free beam demonstrating these methods. Section IV presents the conclusions drawn.

II. DERIVING ROTATIONAL MOBILITIES FROM TRANSLATIONAL MOBILITIES

A. Rotational Velocity/Force Mobility

Figure 2.1(a) depicts a segment of a structure which is being driven by a sinusoidal translational force applied to Point A and in which the resultant sinusoidal translational velocity is being measured at Point B. Considering momentarily that the excitation is at a particular frequency ω_M, the value of the translational mobility at that frequency is the complex quantity $\dot{W}_B(\omega_M)/F_A(\omega_M)$. Now suppose that the velocity measurement is made in turn at each point of a set of points adjacent to Point B with the excitation maintained at Point A as shown in Figure 2.1(b). The resulting complex amplitude ratios $\dot{W}(\omega_M;\eta)/F_A(\omega_M)$ could be plotted as functions of the position coordinate, η, of the measuring point as shown in Figure 2.1(c). The real and imaginary mobility data, if carefully measured, would be found to lie on smooth curves by virtue of the continuity of the wave fields comprising the vibration of the structure. Tangent lines could be drawn to these curves at the coordinate X_B of Point B. The slopes of these tangents would have the following significance. The instantaneous angular displacement of the structure at a location η relative to its rest position would be given by:

$$\theta = \frac{dw}{d\eta} \; .$$

The time rate of change of this slope would be given by:

$$\dot{\theta} = \frac{d}{dt}\frac{dw}{d\eta} = \frac{d}{d\eta}\frac{dw}{dt} = \frac{d}{d\eta}\dot{w} \quad . \tag{2.1}$$

But, because the excitation is sinusoidal, this angular velocity could be expressed as

$$\dot{\theta} = \dot{\Theta}(\omega_M)e^{i\omega_M t} \quad . \tag{2.2}$$

By combining Eq. (2.2) and the relation

$$\dot{w} = \dot{W}(\omega_M;\eta)e^{i\omega_M t}$$

with Eq. (2.1), it is found that

$$\dot{\Theta}(\omega_M;\eta) = \frac{d}{d\eta}\dot{W}(\omega_M;\eta) \quad , \tag{2.3}$$

from which is formed the ratio of complex amplitudes

$$\frac{\dot{\Theta}_B(\omega_M)}{F_A'(\omega_M)} = \frac{d}{d\eta}\frac{\dot{W}(\omega_M;\eta)}{F_A'(\omega_M)}\bigg|_{\eta=x_B}$$
$$= \left\{\frac{d}{d\eta}Re\left[\frac{\dot{W}(\omega_M;\eta)}{F_A'(\omega_M)}\right] + i\frac{d}{d\eta}Im\left[\frac{\dot{W}(\omega_M;\eta)}{F_A'(\omega_M)}\right]\right\}\bigg|_{\eta=x_B} \quad . \tag{2.4}$$

If the indicated measurements and calculations are performed at intervals over a band of driving frequencies, ω , of interest, the rotational velocity/force mobility function is thus derived from the translational mobility symbolically as

$$Y_{\theta_B F_A}(\omega) = \frac{d}{d\eta}Y_{wF_A}(\omega;\eta) \quad . \tag{2.5}$$

B. Translational Velocity/Moment Mobility

In Figure 2.2(a) the structure is again shown with translational excitation and response vectors at Points A and B, respectively. Again with the excitation frequency set at ω_M, suppose that the excitation force is applied in turn at each of a set of points adjacent to A with responses measured at Point B as shown in Figure 2.2(b). The resulting complex amplitude ratios $\dot{W}_B(\omega_M)/F(\omega_M;\xi)$ could be plotted as functions of the position coordinate, ξ, of the excitation point as shown in Figure 2.2(c). The real and imaginary mobility components would again be found to lie on smooth curves to which tangent lines could be drawn at the coordinate x_A of Point A. The significance of the tangent slopes to these curves is explained as follows.

With reference to Figure 2.2(d) it is seen that an instantaneous moment applied to the structure at Point A could be equivalently represented as a pair of equal and opposite parallel forces separated a small distance, ϵ. The response of the structure at Point B to a sinusoidally varying moment at Point A could then be expressed as follows:

$$\dot{w}_B = \dot{W}_B(\omega_M)e^{i\omega_M t} = \lim_{\epsilon \to 0}\left\{\left.\frac{\dot{W}_B(\omega_M)}{F(\omega_M;\xi)}\right|_{\xi = x_A+\epsilon} P(\omega_M)e^{i\omega_M t} - \left.\frac{\dot{W}_B(\omega_M)}{F(\omega_M;\xi)}\right|_{\xi = x_A} P(\omega_M)e^{i\omega_M t}\right\} \quad . \qquad (2.6)$$

Then

$$\dot{W}_B(\omega_M) = \lim_{\epsilon \to 0} \left\{ \frac{\left.\frac{\dot{W}_B(\omega_M)}{F(\omega_M;\xi)}\right|_{\xi = x_A+\epsilon} - \left.\frac{\dot{W}_B(\omega_M)}{F(\omega_M;\xi)}\right|_{\xi = x_A}}{\epsilon} \cdot P(\omega_M)\epsilon \right\}$$

$$= \left.\frac{d}{d\xi}\frac{\dot{W}_B(\omega_M)}{F(\omega_M;\xi)}\right|_{\xi = x_A} \cdot M_A(\omega_M) \quad , \qquad (2.7)$$

from which is formed the ratio of complex amplitudes

$$\frac{\dot{W}_B(\omega_M)}{M_A(\omega_M)} = \left.\frac{d}{d\xi}\frac{\dot{W}_B(\omega_M)}{F(\omega_M;\xi)}\right|_{\xi = x_A}$$

$$= \left\{\frac{d}{d\xi} Re\left[\frac{\dot{W}_B(\omega_M)}{F(\omega_M;\xi)}\right] + i\frac{d}{d\xi} Im\left[\frac{\dot{W}_B(\omega_M)}{F(\omega_M;\xi)}\right]\right\}\Bigg|_{\xi = x_A} . \qquad (2.8)$$

If this ratio is evaluated over a band of driving frequencies, ω, of interest, the translational velocity/moment mobility function is thus derived from the translational mobility symbolically as

$$Y_{W_B M_A}(\omega) = \frac{d}{d\xi} Y_{W_B F}(\omega;\xi) \quad . \qquad (2.9)$$

C. Rotational Velocity/Moment Mobility

The structure will again be envisioned as being excited by a sinusoidal translational force of frequency ω_M at Point A. If the location coordinate ξ of the force application point is then made to vary about x_A, the resultant derivative of translational mobility relates the complex amplitude of translational velocity at Point B to the complex amplitude of applied moment at Point A in accordance with Eq. (2.7). If Eq. (2.3) is written for the case $\eta = x_B$ and is combined with Eq. (2.7), the result

$$\frac{\dot{\Theta}_B(\omega_M)}{M_A(\omega_M)} = \frac{\partial}{\partial \eta} \frac{\partial}{\partial \xi} \frac{\dot{W}(\omega_M;\eta)}{F(\omega_M;\xi)} \Bigg|_{\substack{\eta = x_B \\ \xi = x_A}}$$

$$= \left\{ \frac{\partial^2}{\partial \eta \partial \xi} Re\left[\frac{\dot{W}(\omega_M;\eta)}{F(\omega_M;\xi)}\right] + i \frac{\partial^2}{\partial \eta \partial \xi} Im\left[\frac{\dot{W}(\omega_M;\eta)}{F(\omega_M;\xi)}\right] \right\} \Bigg|_{\substack{\eta = x_B \\ \xi = x_A}} \tag{2.10}$$

is obtained. If this ratio is evaluated over a band of driving frequencies of interest, the rotational velocity/moment mobility function is thus derived from the translational mobility symbolically as:

$$Y_{\theta_B M_A}(\omega) = \frac{\partial^2}{\partial \eta \partial \xi} Y_{WF}(\omega;\eta,\xi) \, . \tag{2.11}$$

D. <u>Summary of Derivative Relationships</u>

The mobility matrix relating the translational and rotational velocity amplitudes at the response measuring Point B to the amplitudes of force and moment at the excitation Point A on a structure was shown in Figure 1.1(e). In accordance with Eqs. (2.5), (2.9) and (2.11) each element of this mobility matrix is a function which can be re-expressed in terms of the translational velocity/force mobility function, yielding the following:

$$\begin{Bmatrix} \dot{W}_B(\omega) \\ \dot{\Theta}_B(\omega) \end{Bmatrix} = \begin{bmatrix} Y_{W_B F_A}(\omega) & Y_{W_B M_A}(\omega) \\ Y_{\theta_B F_A}(\omega) & Y_{\theta_B M_A}(\omega) \end{bmatrix} \begin{Bmatrix} F_A(\omega) \\ M_A(\omega) \end{Bmatrix}$$

$$= \left. \begin{bmatrix} Y_{WF}(\omega;\eta,\xi) & \frac{\partial}{\partial\xi} Y_{WF}(\omega;\eta,\xi) \\ \frac{\partial}{\partial\eta} Y_{WF}(\omega;\eta,\xi) & \frac{\partial^2}{\partial\eta\partial\xi} Y_{WF}(\omega;\eta,\xi) \end{bmatrix} \begin{Bmatrix} F_A(\omega) \\ M_A(\omega) \end{Bmatrix} \right|_{\substack{\eta = x_B \\ \xi = x_A}} \tag{2.12}$$

or, using more compact notation,

$$\begin{Bmatrix} \dot{W}_B \\ \dot{\Theta}_B \end{Bmatrix} = \begin{bmatrix} Y_{W_B F_A} & \frac{\partial}{\partial\xi} Y_{W_B F_A} \\ \frac{\partial}{\partial\eta} Y_{W_B F_A} & \frac{\partial^2}{\partial\eta\partial\xi} Y_{W_B F_A} \end{bmatrix} \begin{Bmatrix} F_A \\ M_A \end{Bmatrix} . \tag{2.13}$$

It is emphasized that each element in the mobility matrix represents a function of angular frequency ω defined over some band of interest.

E. Implementation by Finite Difference Method

The calculation of spatial derivatives of translational velocity/force mobilities is the essence of the above described approach to determining rotational mobilities. For application of this approach to the experimental determination of mobilities, these derivatives must be approximated from conventional mobility measurements made at a limited number of discrete locations on a structure. The method of finite differences, References (10) and (11), is used for this purpose.

Let the symbol ψ denote a translational velocity/force mobility function to identify it as one of a set of conventional mobilities from which one or more rotational mobilities will be derived. These conventional mobilities will be determined with response velocity measurements made at locations $\ldots, \eta_{m-1}, \eta_m, \eta_{m+1}, \ldots$ spaced $\Delta\eta$ apart, and with force excitations applied at locations $\ldots, \xi_{n-1}, \xi_n, \xi_{n+1}, \ldots$ spaced $\Delta\xi$ apart. Thus the notation $\psi_{m,n}$ will represent the mobility function $\psi(\omega; \eta_m, \xi_n)$.

If ψ were a function of only the single spatial coordinate η, each of the following expressions would approximate the continuous ordinary first derivative of that function, correct to within truncation errors of the order of $(\Delta\eta)^2$:

$$\text{Central Difference: } \left.\frac{d\psi}{d\eta}\right|_{\eta_m} \approx \frac{\psi_{m+1} - \psi_{m-1}}{2\Delta\eta}$$

$$\text{Forward Difference: } \left.\frac{d\psi}{d\eta}\right|_{\eta_m} \approx \frac{-3\psi_m + 4\psi_{m+1} - \psi_{m+2}}{2\Delta\eta} \qquad (2.14)$$

$$\text{Backward Difference: } \left.\frac{d\psi}{d\eta}\right|_{\eta_m} \approx \frac{3\psi_m - 4\psi_{m-1} + \psi_{m-2}}{2\Delta\eta}$$

The choice of the approximation which would be used from among these three would depend on whether the location η_m where the derivative is desired happens to be an inboard location, and if an end location, whether at the positive end or the negative end of the η interval. For the mobility function $\psi(\omega; \eta, \xi)$ in which two spatial coordinates are involved, the first partial derivative approximations have similar form to the ordinary derivative approximation:

Central Difference:

$$\left.\frac{\partial\psi}{\partial\eta}\right|_{\eta_m,\xi_n} \approx \frac{\psi_{m+1,n}-\psi_{m-1,n}}{2\Delta\eta}\ ;\ \left.\frac{\partial\psi}{\partial\xi}\right|_{\eta_m,\xi_n} \approx \frac{\psi_{m,n+1}-\psi_{m,n-1}}{2\Delta\xi}$$

Forward Difference:

$$\left.\frac{\partial\psi}{\partial\eta}\right|_{\eta_m,\xi_n} \approx \frac{-3\psi_{m,n}+4\psi_{m+1,n}-\psi_{m+2,n}}{2\Delta\eta}\ ;\ \left.\frac{\partial\psi}{\partial\xi}\right|_{\eta_m,\xi_n} \approx \frac{-3\psi_{m,n}+4\psi_{m,n+1}-\psi_{m,n+2}}{2\Delta\xi} \tag{2.15}$$

Backward Difference:

$$\left.\frac{\partial\psi}{\partial\eta}\right|_{\eta_m,\xi_n} \approx \frac{3\psi_{m,n}-4\psi_{m-1,n}+\psi_{m-2,n}}{2\Delta\eta}\ ;\ \left.\frac{\partial\psi}{\partial\xi}\right|_{\eta_m,\xi_n} \approx \frac{3\psi_{m,n}-4\psi_{m,n-1}+\psi_{m,n-2}}{2\Delta\xi}$$

The latter expressions are directly usable in evaluating the rotational velocity/force mobility and the translational velocity/moment mobility as indicated in Eqs.(2.12) and (2.13) given that $\eta_m = X_B$ and $\xi_n = X_A$, or $\psi_{m,n} = Y_{W_B F_A}$.

The mixed second partial derivative can be approximated by one of the following expressions:

Central Difference:

$$\left.\frac{\partial^2\psi}{\partial\eta\partial\xi}\right|_{\eta_m,\xi_n} \approx \frac{\psi_{m+1,n+1}-\psi_{m+1,n-1}-\psi_{m-1,n+1}+\psi_{m-1,n-1}}{4\Delta\eta\Delta\xi}$$

Forward Difference:

$$\left.\frac{\partial^2\psi}{\partial\eta\partial\xi}\right|_{\eta_m,\xi_n} \approx \frac{1}{4\Delta\eta\Delta\xi}\Big[9\psi_{m,n}-12\psi_{m,n+1}+3\psi_{m,n+2} \tag{2.16}$$
$$-12\psi_{m+1,n}+16\psi_{m+1,n+1}-4\psi_{m+1,n+2}+3\psi_{m+2,n}-4\psi_{m+2,n+1}+\psi_{m+2,n+2}\Big]$$

Backward Difference:

$$\left.\frac{\partial^2\psi}{\partial\eta\partial\xi}\right|_{\eta_m,\xi_n} \approx \frac{1}{4\Delta\eta\Delta\xi}\Big[9\psi_{m,n}-12\psi_{m,n-1}+3\psi_{m,n-2}-12\psi_{m-1,n}$$
$$+16\psi_{m-1,n-1}-4\psi_{m-1,n-2}+3\psi_{m-2,n}-4\psi_{m-2,n-1}+\psi_{m-2,n-2}\Big] \quad \text{(2.16 cont'd)}$$

The above central difference expression is usable for evaluating any rotational velocity/moment mobility in which the hypothetical moment excitation is applied at a point inboard of the ends and the rotational velocity response is at the same point or any other inboard point. The forward difference expression applies only to the case in which both η_m and ξ_n coincide with the negative ends of their ranges; i.e., the hypothetical moment excitation is applied and the rotational velocity response is measured at the left end of the structure. Similarly, the backward difference expression applies only in the case where both the hypothetical moment excitation and the rotational velocity response locations are at the right (positive) end of the structure. Such end-located rotational mobilities would be of main importance in analyzing the dynamic response of cantilevered structures. However, in instances where the moment excitation would be applied at an end point and the rotational velocity response would be measured at some other location, or vice-versa, none of the above difference expressions would be applicable. Reference (11) contains other finite difference formulations which would apply in these instances.

In summary, the evaluation of a particular rotational mobility using the above finite difference approximation methods requires the prior determination of between two and nine conventional translational mobilities, the quantity depending on the location and type of rotational mobility desired. For driving point rotational velocity/moment mobilities the number of translational mobilities needed may be cut almost in half by resort to the use of the reciprocal theorem for dynamic loads, Reference (12); because $\psi_{m,n} = \psi_{n,m}$ as a consequency of this theorem, either of these mobilities may be substituted for the other. It is further noted that several different rotational mobilities can be evaluated using a common set of translational mobilities.

The selection of response measurement and excitation location spacings, $\Delta\eta$ and $\Delta\xi$, must achieve a balance between resolution and proper approximation of derivatives across the number of natural modes of vibration encompassed in the band of frequencies. Some analytically or experimentally obtained knowledge of mode shapes is desirable for use in the determination of the point spacings. The results of Section III.D demonstrate that this balance is achievable with latitude in the selection, at least in cases where a limited number of resonances are included in the frequency band.

III. EXPERIMENTAL MOBILITY MEASUREMENTS ON A FREE-FREE BEAM

A. Test Specimen and Test Equipment

Figure 3.1 depicts the beam which was prepared from cold rolled steel rectangular bar stock for experiments to demonstrate the previously described approach to obtaining rotational mobilities. Excitation point and motion monitoring point locations were established for experimental measurements of all the conventional translational mobilities needed to generate the rotational mobilities identified in Figure 3.2 by the methods of backward differences. The mobilities included therein would be among those required to predict the translational motion at Point A due to cantilever attachment of the beam to a moving foundation or other component at Point B.

The particular set of beam cross section dimensions was chosen such that the off-axis (stiff direction) natural vibration frequencies would not coincide with the drive direction (flexible direction) natural frequencies. The tapped holes shown in Figure 3.1 were added to enable stud attachment of an impedance head for force measurements at each drive point location in turn. Because most of the required translational mobilities were to be transfer mobilities, all motion measurements were made by attaching the accelerometer to the opposite side of the beam from the impedance head using beeswax. Accurate placement of the accelerometer was facilitated by lines scribed on the surface coincident with the driving stud hole centers. It is seen in Figure 3.1 that the outermost drive points were located as close to the beam ends as possible with assurance of proper seating of the instrumentation at these end locations. The .044m spacing of the driving and measuring points at End B was established by first sketching the mode shape of the expected highest resonance within the planned test frequency band of 0-2000 Hz. The three driving points were then spaced at the widest distance where the backward difference method could be expected to approximate the slope of this mode shape reasonably well. This spacing was chosen as wide as possible to provide resolution for accuracy in the approximation of slopes at the frequency of the lowest resonance.

The mobility tests were conducted using broad band stationary random excitation. The force and acceleration signals were recorded and processed by a minicomputer using the fast Fourier transform coherence/cross spectral density program COHER previously developed for the Acoustics and Vibration Laboratory in conjunction with the Reference (5) ScD dissertation. The overall test system with identification of the test equipment used is shown in Figure 3.3.

The test beam, which weighed 5.64 kg, was suspended vertically from one end by means of elastic bands and was driven horizontally to effect the intended free-free boundary conditions. The horizontally oriented shaker, which was capable of generating a maximum force amplitude of about 25 nt, was connected to the stud-mounted impedance head by means of a .05m long by .002m diameter shaft capble of accommodating minor misalignments between shaker and beam. The beeswax-mounted accelerometer was of 2 grams mass, and the total mass of the impedance head was 60 grams.

B. Test Procedure

Calibration of the accelerometer signal channel was performed by temporarily mounting the accelerometer on a General Radio Model 1557A calibrator. Subsequently, the force signal channel was calibrated by connecting a rigid disk of known mass to the impedance head and exciting it sinusoidally; the calibrated accelerometer signal and the known mass were used to establish the actual force amplitude represented by a given force signal. The calibration values obtained were found to be close to the transducer manufacturers' ratings. The proper functioning of the entire test system was later verified by driving the rigid disk with random force input; the mobility data generated by the system were matched very closely by the theoretical mobility of a pure mass of the same value.

To maximize the dynamic range of the measurement system, it was necessary to make the frequency spectrum of both channels simultaneously as flat as possible across the 0-2000 Hz band of interest. The test beam was instrumented at typical driving and response locations, and the signal spectra were monitored in real time using the spectrum analyzer. It was found that adequate flatness could be obtained with the use of one signal generator output bandpass filter as shown in Figure 3.3. A 63 Hz high pass corner frequency setting and a 1600 Hz low pass corner frequency setting were used for this filter throughout the beam mobility testing. These settings provided the required flatness of signal spectra from 0 to 2000 Hz while providing desired roll-off in driving force above 2000 Hz and precluding large-amplitude,low-frequency rigid body motions of the beam.

Prior to the start of each mobility data acquisition run the signal channel gains were adjusted until the signal levels, monitored on the oscilloscope, seldom exceeded the 5 volt maximum input level of the analog to digital converters. The channel gain values and transducer sensitivity values were then specified as input data to the computer along with the desired number of averages (400 for each run). Also specified was the maximum frequency value (one-half the sampling rate), which was 2560 Hz for all runs. The force and acceleration signal channel bandpass filters were accordingly set at corner frequencies of 2 Hz (high pass) and 2000 Hz (low pass) for both channels. The latter setting was consistent with the Reference (5) recommendation that the high frequency roll-off point be set at 0.4 times the sampling rate to eliminate aliasing effects.

C. Measured Vs. Theoretical Translational Mobilities

For each mobility test run, the minicomputer calculated power spectral densities and cross spectral densities of the force and acceleration signals along with their relative phase and coherence values. These outputs were generated at discrete frequencies spaced 10 Hz apart over a band extending from 10 Hz to 2000 Hz and were converted into translational mobilities as explained below.

In the definition of a translational mobility as a transfer function relating sinusoidal force and velocity quantities, the acceleration corresponding to the velocity $\dot{w} = \dot{W}e^{i\omega t}$ is given as

$$\ddot{w} = i\omega\dot{W}e^{i\omega t} = Ae^{i\omega t}. \tag{3.1}$$

Then the translational mobility is related to the acceleration/force cross spectral density, G_{AF}, and the power spectral density of the force, G_{FF}, in accordance with

$$\psi = \frac{\dot{W}}{F} = \frac{1}{i\omega}\frac{A}{F} = \frac{1}{i\omega}\frac{G_{AF}}{G_{FF}} = \frac{1}{\omega}\frac{G_{AF}}{G_{FF}}e^{-i\frac{\pi}{2}}. \tag{3.2}$$

Separating these complex quantities into their magnitude and phase components, we obtain

$$\left|\frac{\dot{W}}{F}\right|e^{i\phi} = \frac{1}{\omega}\frac{|G_{AF}|}{G_{FF}}e^{i(\phi_{AF}-\frac{\pi}{2})}, \tag{3.3}$$

where ϕ_{AF} is the phase angle of the complex cross spectral density G_{AF}. The magnitude portion of Eq.(3.3)can be re-expressed in terms of the frequency and spectral density quantities in the form output by the COHER program:

$$10^{\log_{10}\left|\frac{\dot{W}}{F}\right|} = 10^{\left[\log_{10}|G_{AF}| - \log_{10} G_{FF} - \log_{10}\omega\right]}, \tag{3.4}$$

which yields

$$20\log_{10}\left|\frac{\dot{W}}{F}\right| = 2\left[10\log_{10}|G_{AF}| - 10\log_{10}G_{FF}\right] - 20\log_{10}(2\pi f) \tag{3.5}$$

The phase portion of (3.3) is simply

$$\phi = \phi_{AF} - 90^{\circ}. \tag{3.6}$$

Frequently the force and acceleration signals in mobility measurements are corrected for the mass and flexibility effects of the portion of the impedance head below the force gage. Such corrections are described in Reference (5), but the corrections therein pertain to driving point mobilities only. In transfer mobility measurements these effects cannot be determined with the test system described, as the measured accelerations are different from those sustained by the impedance head. Because the bulk of the mobilities measured were transfer mobilities, no impedance head corrections were made in any of the runs.

The computer program TRANS, listed in Appendix C, was written to convert the spectral density output data from COHER into translational mobilities per Eqs.(3.5) and (3.6) and to create plots and store the results in quadrature form on disk for later manipulation. Data input to the TRANS program is via punched cards. A separate program, THEOR, listed in Appendix B, was written to generate theoretical translational and rotational mobility functions for Bernoulli-Euler beams and to store them on disk in magnitude and phase form for use in comparison with the experimental results. The derivation of the equations programmed in THEOR is presented in Appendix A.

By virtue of the reciprocal theorem for dynamic loads, Reference (12), mobility matrices such as given in Figure 3.2 are symmetric. Thus all elements of the matrix shown would be established if only the upper or lower triangular portion were evaluated. If arbitrarily the lower triangular portion is chosen to be evaluated, the translational mobilities needed to establish this matrix are as follows:

$$Y_{W_A F_A}(\omega): \psi_{1,1} \qquad Y_{\theta_B F_A}(\omega): \psi_{4,1}, \psi_{3,1}, \psi_{2,1}$$

$$Y_{W_B F_A}(\omega): \psi_{4,1} \qquad Y_{\theta_B F_B}(\omega): \psi_{4,4}, \psi_{3,4}, \psi_{2,4}$$

$$Y_{W_B F_B}(\omega): \psi_{4,4} \qquad Y_{\theta_B M_B}(\omega): \psi_{4,4}, \psi_{4,3}, \psi_{4,2}, \psi_{3,4}, \psi_{3,3}, \psi_{3,2}, \psi_{2,4}, \psi_{2,3}, \psi_{2,2}.$$

A further consequence of the reciprocal theorem is the symmetry of translational mobilities, i.e., $\psi_{m,n} = \psi_{n,m}$. Also, by geometric symmetry it is seen that $\psi_{1,1} = \psi_{4,4}$. Combining these commonalities, the entire nine-element mobility matrix shown in Figure 3.2 would be established by measurement of the following nine translational mobilities or their reciprocals:

$$\psi_{1,2}, \psi_{1,3}, \psi_{1,4}, \psi_{2,2}, \psi_{2,3}, \psi_{2,4}, \psi_{3,3}, \psi_{3,4}, \psi_{4,4} (\text{or } \psi_{1,1}).$$

Theoretical and experimental versions of these translational mobilities were generated as explained above. A tendency toward erratic results was observed in the experimental magnitude data in regions of resonances. It was found that these erratic results occurred at frequencies where the coherence values fell to low levels (less than .50). The low coherences were attributable to the force signal spectra having decayed to the level of the background noise floor at the resonances; this tendency is more pronounced with items having low damping such as the test beam. In an attempt to obtain the best possible translational mobility data for subsequent use in deriving rotational mobilities, replacement magnitude data for the more noticeably erratic regions were obtained using sinusoidal excitation. A sine wave generator was substituted for the random signal generator and bandpass filter, and the acceleration and force signal peak values were read from the oscilloscope without the use of the computer. No revised phase measurements were made. A typical comparison of the original random excitation mboility results with the substituted-data version of the same mobility is shown for $\psi_{4,1}$ in Figure 3.4. Magnitude data substitutions were made in the experimental mobilities as follows:

Mobility	Frequency Range(s) of Substitution
$\psi_{1,2}$	None
$\psi_{3,1}$	330-530, 770-960
$\psi_{4,1}$	300-530, 750-950
$\psi_{2,2}$	None
$\psi_{3,2}$	None
$\psi_{4,2}$	None
$\psi_{3,3}$	130-220, 380-520
$\psi_{4,3}$	330-520
$\psi_{4,4}$	430-540, 790-960

The substitutions were made over wide enough bands of frequencies so that the sinusoidally generated data merged with the random-excitation data with minimal discontinuities.

Figures 3.5 through 3.12 show plots of the substituted data versions of the remaining experimental translational mobilities. All theoretical mobility plots are comprised of straight line segments connecting data points at 10 Hz intervals and are calculated based on an assumed equivalent viscous damping ratio of .005 for each elastic mode. In general, the agreement between the experimental and the theoretical results is good up to the third resonance (approximately 850 Hz); however, there are noticeable discrepancies in frequency at the fourth resonance. The reason for the discrepancies is not clear; possibly the impedance head rotational inertia became significant in this higher mode, where rotational kinetic energy acquired its greatest proportion of the total kinetic energy.

It was concluded that the portions of the experimental data below 1000 Hz could be considered "good" data for generating rotational mobilities, but that satisfactory results could not be expected above 1000 Hz.

D. Experimentally Derived Vs. Theoretical Rotational Mobilities

The computer program ROTAT listed in Appendix D was written to perform the backward difference calculations indicated in Eqs. (2.15) and (2.16), which generate right-end rotational mobilities such as those indicated in Figure 3.2 from an appropriately chosen set of translational mobilities. The translational mobilities are read by the computer from storage on disk in quadrature component form over a set of discrete frequencies. The output rotational mobilities are plotted in magnitude and phase form and can be stored on disk for subsequent manipulation if desired.

The previously discussed experimental translational mobilities were read by this program for calculation of the test beam rotational mobilities $Y_{\theta_B F_A}(\omega)$, $Y_{\theta_B F_B}(\omega)$, and $Y_{\theta_B M_B}(\omega)$. The results are shown plotted in Figures 3.13, 3.14 and 3.15, respectively, along with corresponding theoretical mobility functions generated with the use of the previously mentioned computer program THEOR. Again a damping ratio value of .005 was used for each elastic mode in calculating the theoretical mobilities.

The agreement between the experimental and theoretical versions of the rotational velocity/force mobilities $Y_{\theta_B F_A}(\omega)$ and $Y_{\theta_B F_B}(\omega)$ over the previously cited 0-1000 Hz band of "good" translational mobility data is reasonably close. Although the experimentally derived rotational velocity/moment mobility $Y_{\theta_B M_B}(\omega)$ gives reasonably clear and accurate indications of resonances, it exhibits a great deal of scatter in both magnitude and phase in some regions. This latter mobility function and its constituent translational mobilities were examined closely in the frequency band 230 to 300 Hz, where there was a marked degree of scatter in both the magnitude and phase plots.

The translational mobility data in this band were generated entirely by random excitation with no substitution of sinusoidally generated data. The scatter in the derived mobility data in this band seems at first glance to be inconsistent with the smoothness of the translational mobility data, Figures 3.4 through 3.12, within the same band. The quadrature components of the constituent translational mobilities over this band are plotted on expanded scales in

Figures 3.16 and 3.17, and the quadrature components of the resultant rotational mobility are shown in Figure 3.18. It is seen that the translational mobilities had been nearly purely imaginary, but the algebraic summation of these numbers gave a resultant imaginary component which was much smaller than most of the individual constituents, magnifying the minor degrees of irregularity present in them. The scatter in the real components of the constituents, Figure 3.16, had been present due to minor deviations in measured phase from the ideal value, -90°. The scatter in the quadrature components of the resultant mobility $Y_{\theta_B M_B}(\omega)$, Figure 3.18, is the source of the scatter in the magnitude and phase noted in Figure 3.15.

This examination of scatter in the $Y_{\theta_B M_B}(\omega)$ mobility shows that the stability of derived rotational mobilities would be enhanced by performing smoothing operations on the translational mobility data before the differencing calculations. An effective approach to smoothing might be to fit analytical mobility expressions to a number of data points in each experimental mobility as described in References (4) and (9). Examples of the resultant rotational mobilities which can be derived by the differencing method from translational mobilities which are smooth and accurate are shown in Figures 3.19 and 3.20. The THEOR program was temporarily modified to establish quadrature versions of the theoretical translational mobilities of Figures 3.4 through 3.12 on disk files, and the

$Y_{\theta_B F_B}(\omega)$ and $Y_{\theta_B M_B}(\omega)$ mobility data points in Figures 3.19 and 3.20 were generated by having the ROTAT program process these files in the same manner as it had processed the experimental data. With the exception of small deviations in antiresonant frequencies seen in Figure 3.20, the agreement between the theoretical and derived mobilities is excellent.

Figures 3.21 through 3.24 show $Y_{\theta_B F_B}(\omega)$ and $Y_{\theta_B M_B}(\omega)$ rotational mobility results similarly derived from theoretical translational mobilities which were calculated at locations corresponding to $\Delta\eta = \Delta\xi = .088m$ and $\Delta\eta = \Delta\xi = .022m$, or twice and one-half the spacing of the experimental measurement points. The results for the wide spacing, Figures 3.21 and 3.22, show additional degrees of the antiresonant frequency deviation noted in Figure 3.20, but the more important matching of resonant frequencies is again achieved. The results for close spacing, Figures 3.23 and 3.24, show excellent agreement throughout. Thus the latitude of the differencing method of deriving rotational mobilities in accommodating variation in measurement location spacings is demonstrated.

IV. CONCLUSIONS

Rotational mobilities of structures are equivalent to spatial derivatives of their translational mobilities and can be determined experimentally by finite difference approximations involving sets of measured translational mobilities. Good agreement was obtained between experimentally and theoretically generated versions of two rotational velocity/force mobilities of a free-free beam. An experimentally derived rotational velocity/moment mobility gave reasonably good indications of resonance, but exhibited large amounts of scatter in some frequency bands. This scatter was found to result from the subtraction of nearly equal translational mobility quantities in the differencing operation, magnifying minor irregularities present in them.

It is believed that this scatter in the rotational mobilities can be eliminated by smoothing operations on the translational mobility data such as curve fitting before the differencing calculations. However, further investigation should be conducted to determine an efficient algorithm for performing the smoothing and to evaluate its effectiveness in reproducing the magnitudes and trends that characterize the experimental data.

It has been shown that the differencing method of determining rotational mobilities can accommodate considerable variation in the spacings of the points where the constituent translational mobilities are measured.

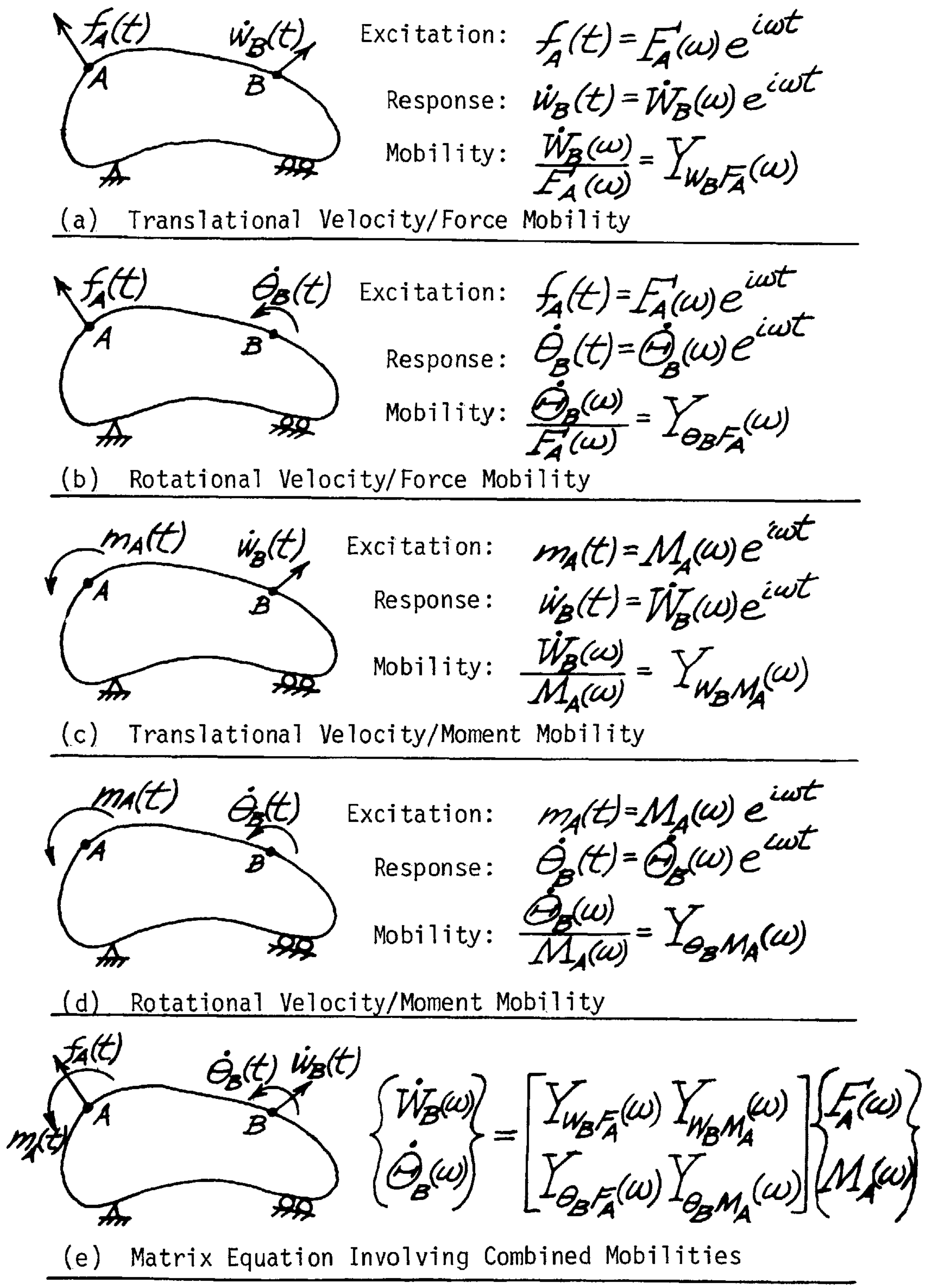

FIGURE 1.1: Transfer Mobilities Involving Various Combinations of Translational and Rotational Effects

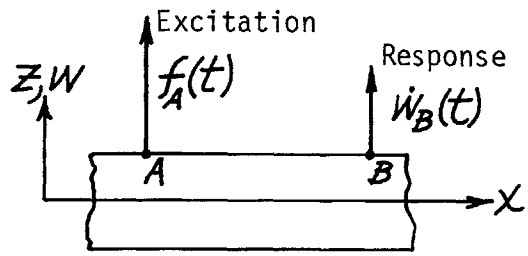

$$f_A(t) = F_A(\omega_M)\, e^{i\omega_M t}$$
$$\dot{w}_B(t) = \dot{W}_B(\omega_M)\, e^{i\omega_M t}$$

(a) Fixed Response Measurement Location

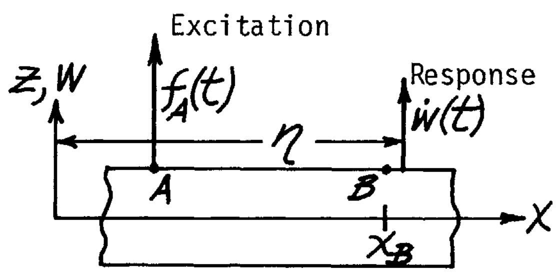

$$f_A(t) = F_A(\omega_M)\, e^{i\omega_M t}$$
$$\dot{w}(t) = \dot{W}(\omega_M;\eta)\, e^{i\omega_M t}$$

(b) Varying Response Measurement Location.

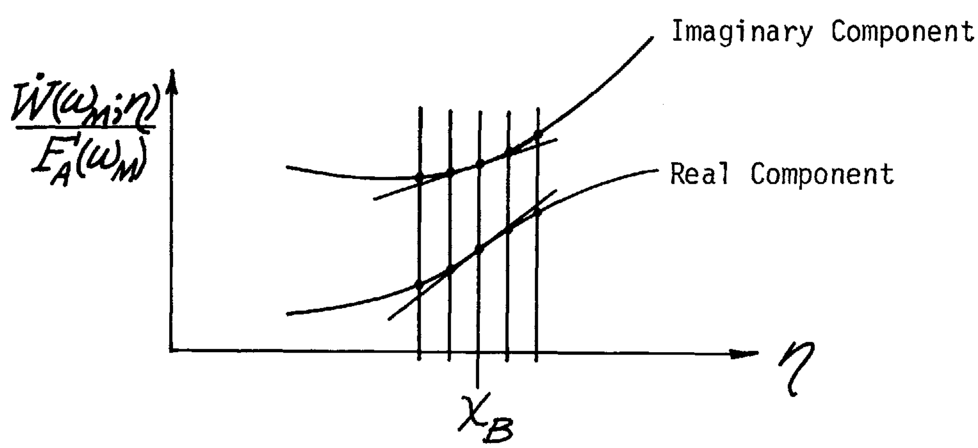

(c) Plot of Resultant Complex Amplitude Ratios

FIGURE 2.1: Relationship of Rotational Velocity/Force Mobility to Translational Mobility at a Single Frequency

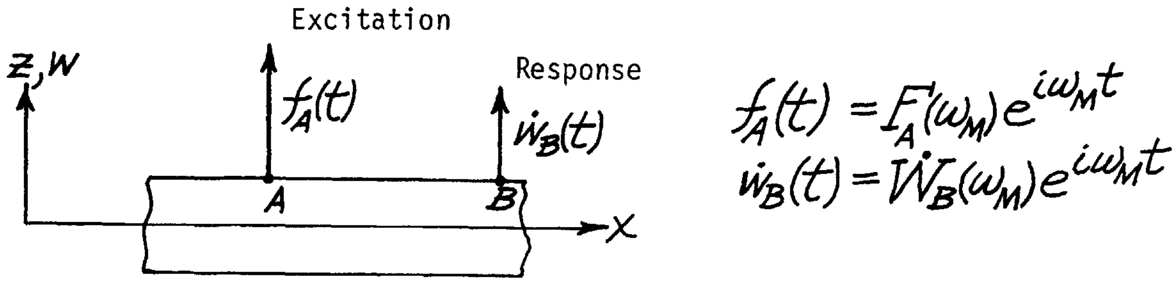

(a) Fixed Excitation Location

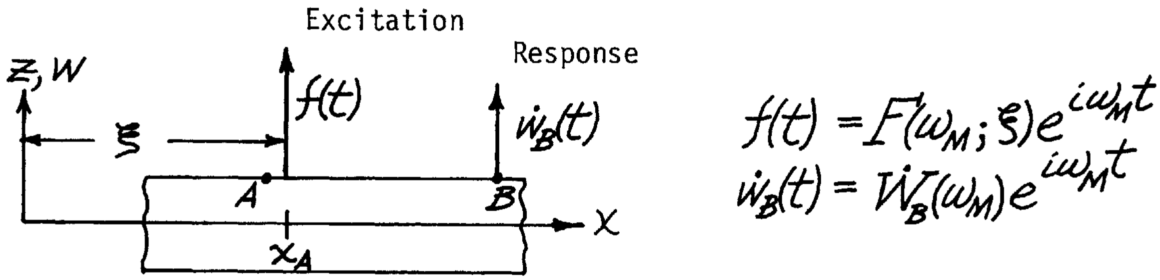

(b) Varying Excitation Location

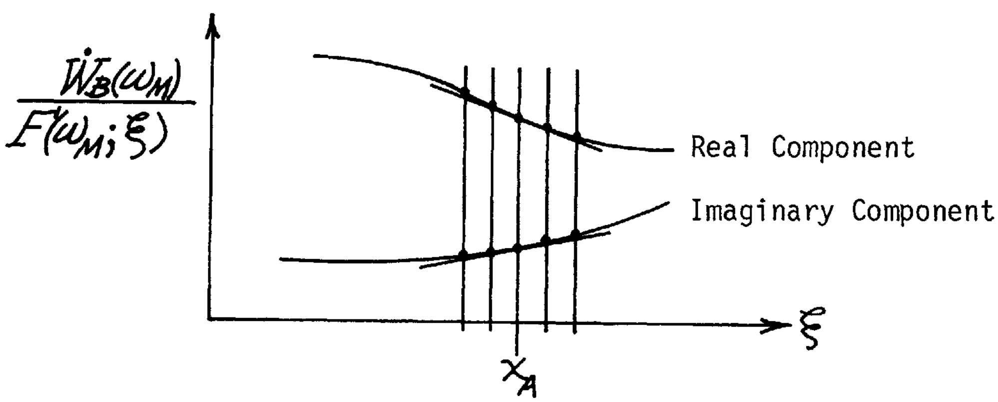

(c) Plot of Resultant Complex Amplitude Ratios

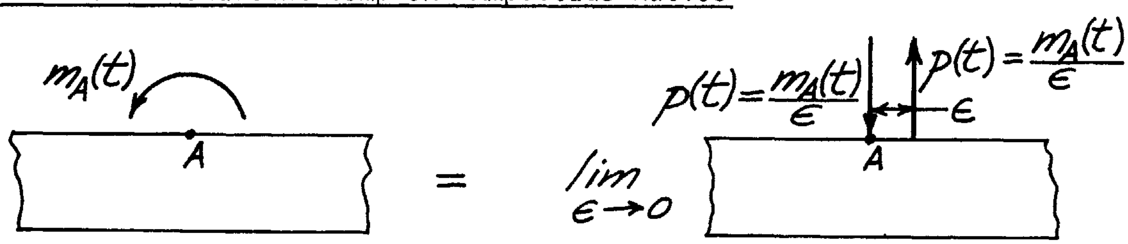

(d) Substitution of Equivalent Force Pair for Moment

FIGURE 2.2: Relationship of Translational Velocity/Moment Mobility to Translational Mobility at a Single Frequency

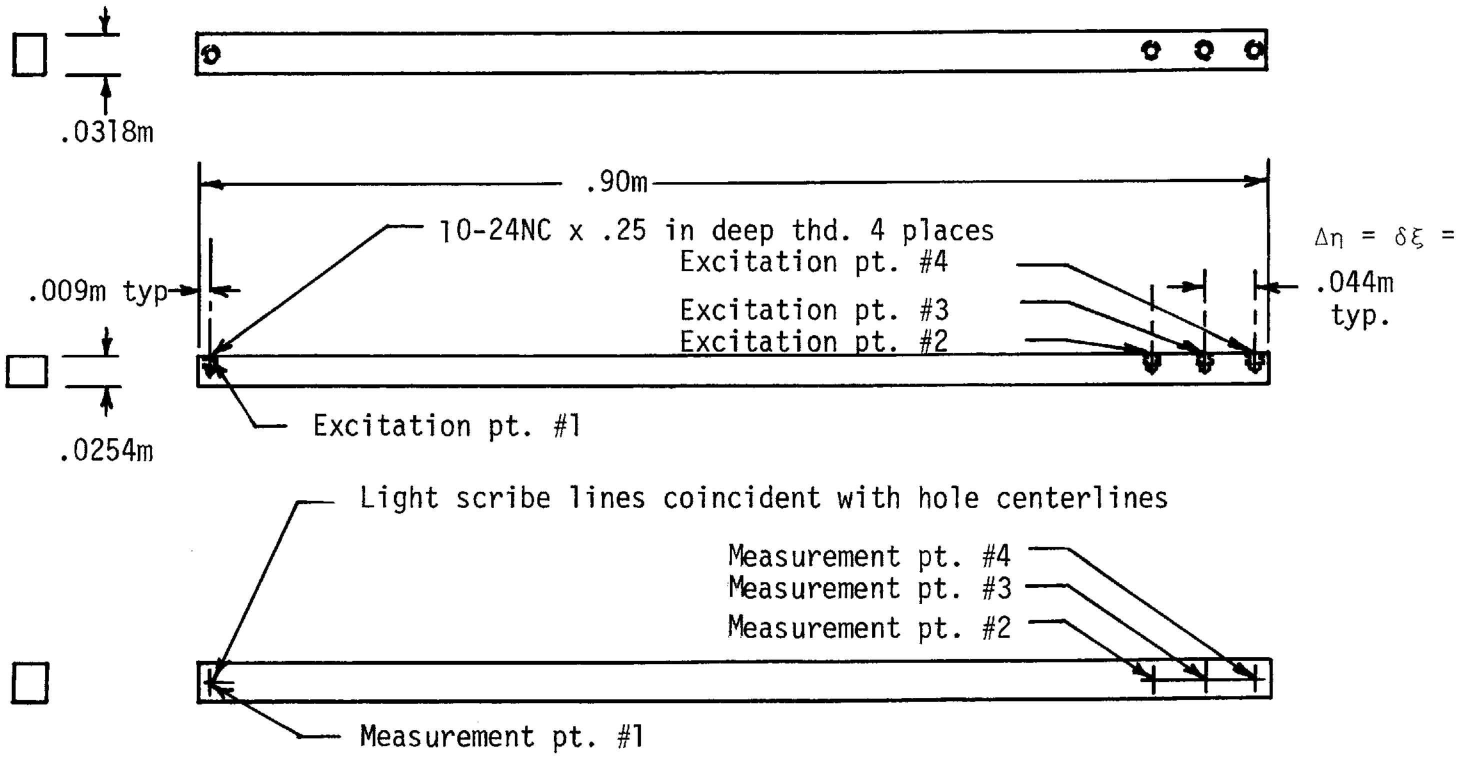

Material: 1.00 in. x 1.25 in. cold rolled steel

FIGURE 3.1: Test Beam Details

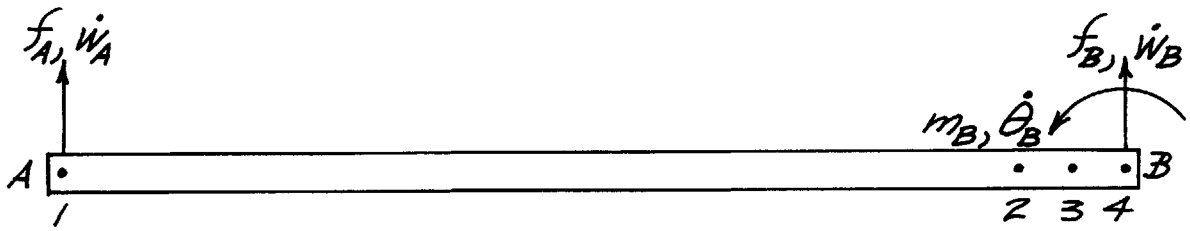

$$
\begin{Bmatrix} \dot{W}_A \\ \dot{W}_B \\ \dot{\Theta}_B \end{Bmatrix} = \begin{bmatrix} Y_{W_A F_A}(\omega) & Y_{W_A F_B}(\omega) & Y_{W_A M_B}(\omega) \\ Y_{W_B F_A}(\omega) & Y_{W_B F_B}(\omega) & Y_{W_B M_B}(\omega) \\ Y_{\theta_B F_A}(\omega) & Y_{\theta_B F_B}(\omega) & Y_{\theta_B M_B}(\omega) \end{bmatrix} \begin{Bmatrix} F_A \\ F_B \\ M_B \end{Bmatrix}
$$

FIGURE 3.2: Matrix of Desired Beam Mobilities

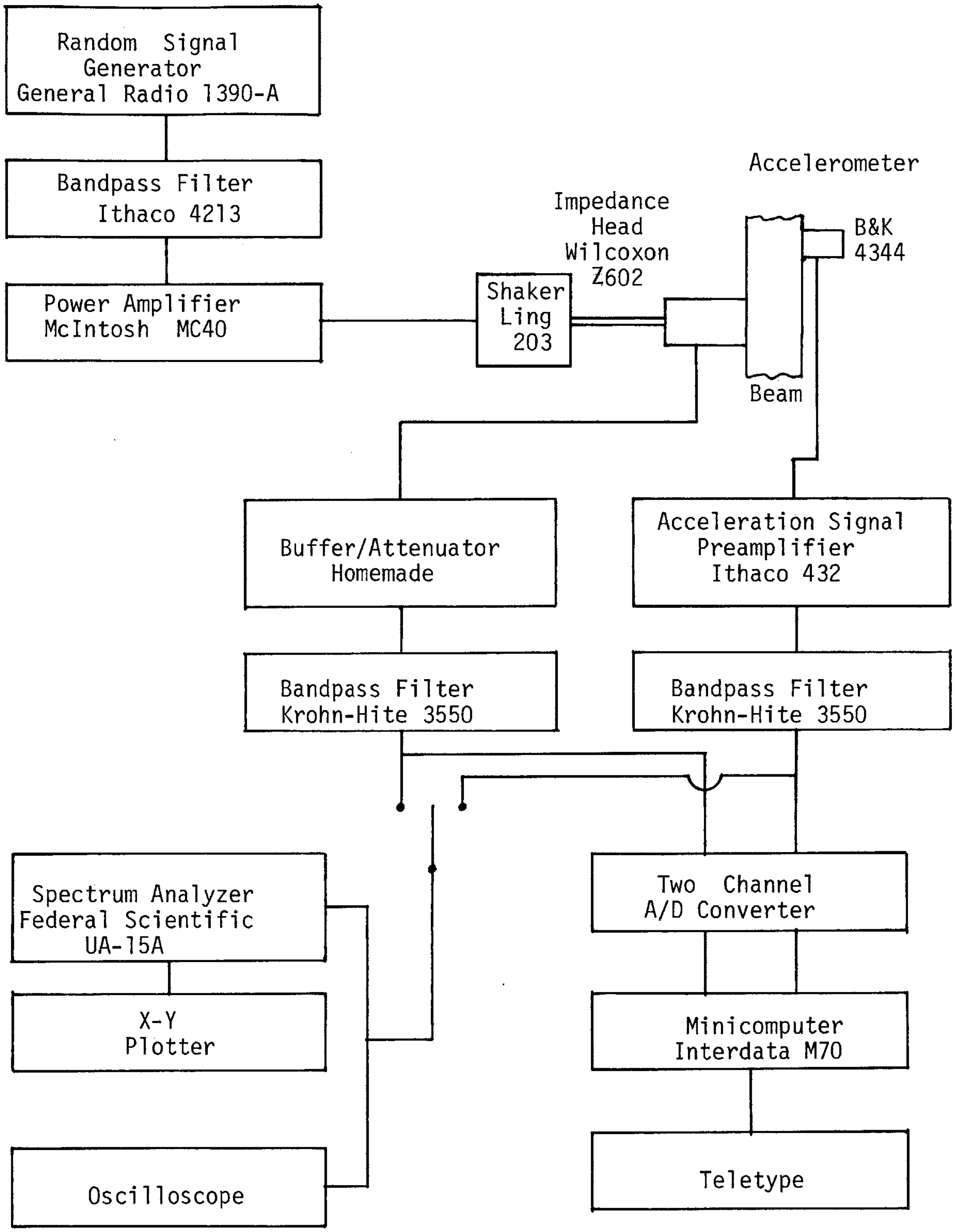

FIGURE 3.3: Test System Schematic Diagram

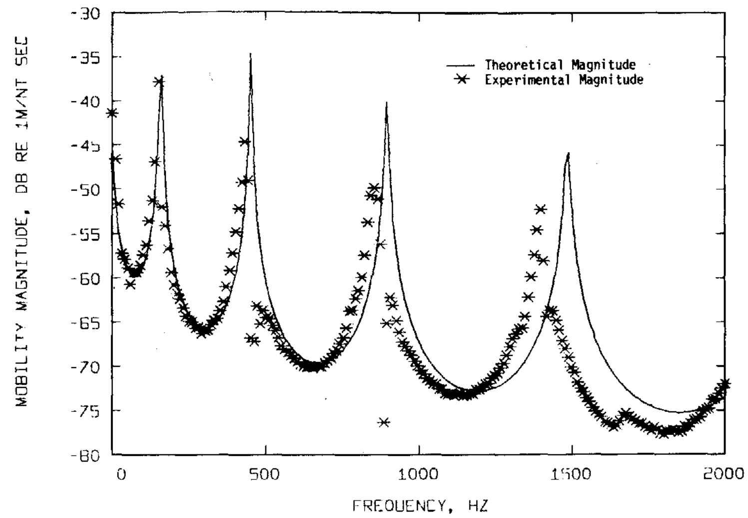

(a) Original Mobility Obtained with Random Excitation

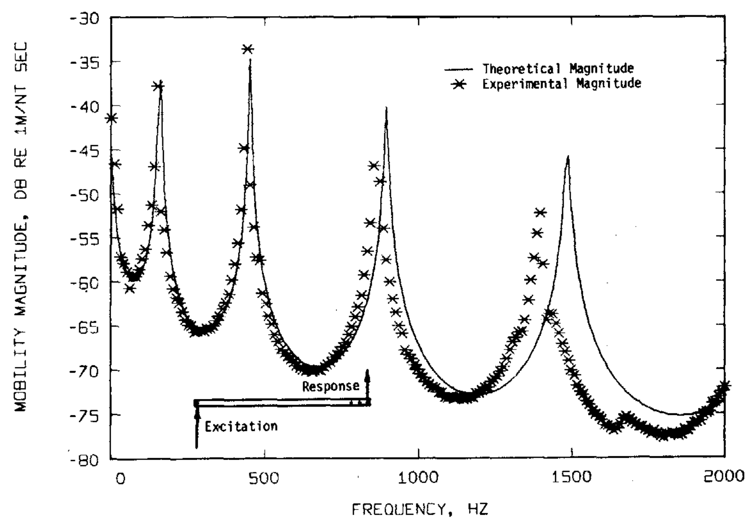

(b) After Substitution of Sinusoidally Generated Data

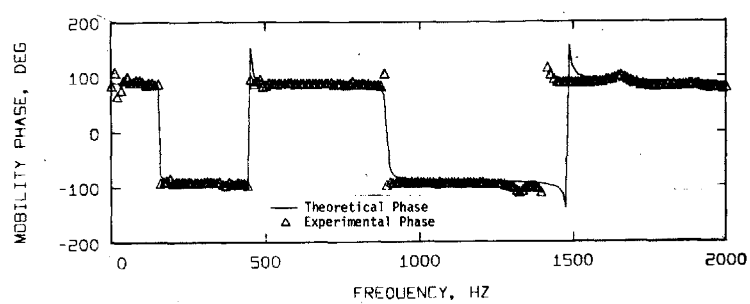

(c) Mobility Phase Plot

FIGURE 3.4: Test Beam Translational Mobility $\psi_{4,1}$ Before and After Data Substitution

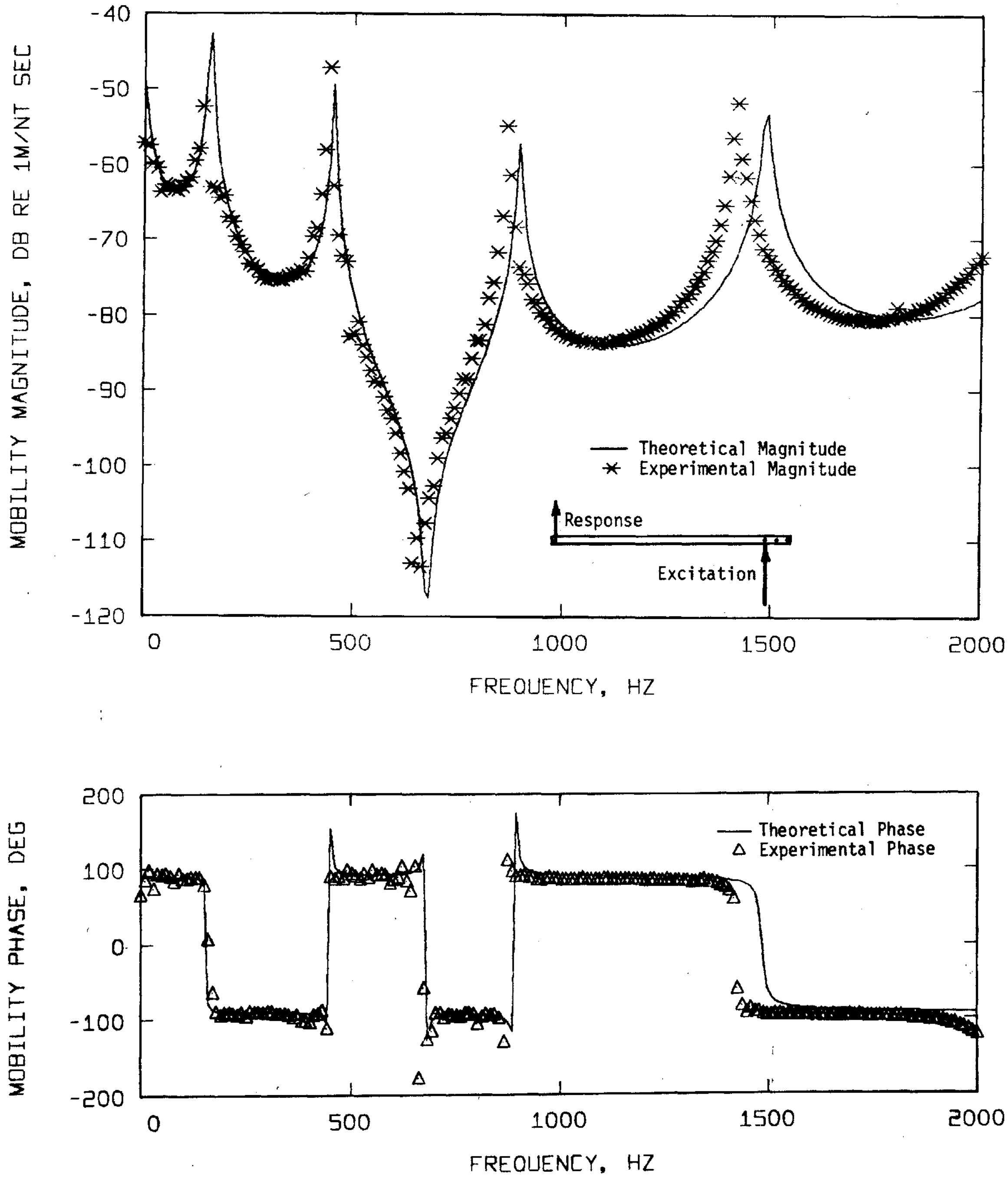

FIGURE 3.5: Test Beam Experimental and Theoretical Translational Mobility $\psi_{1,2}$

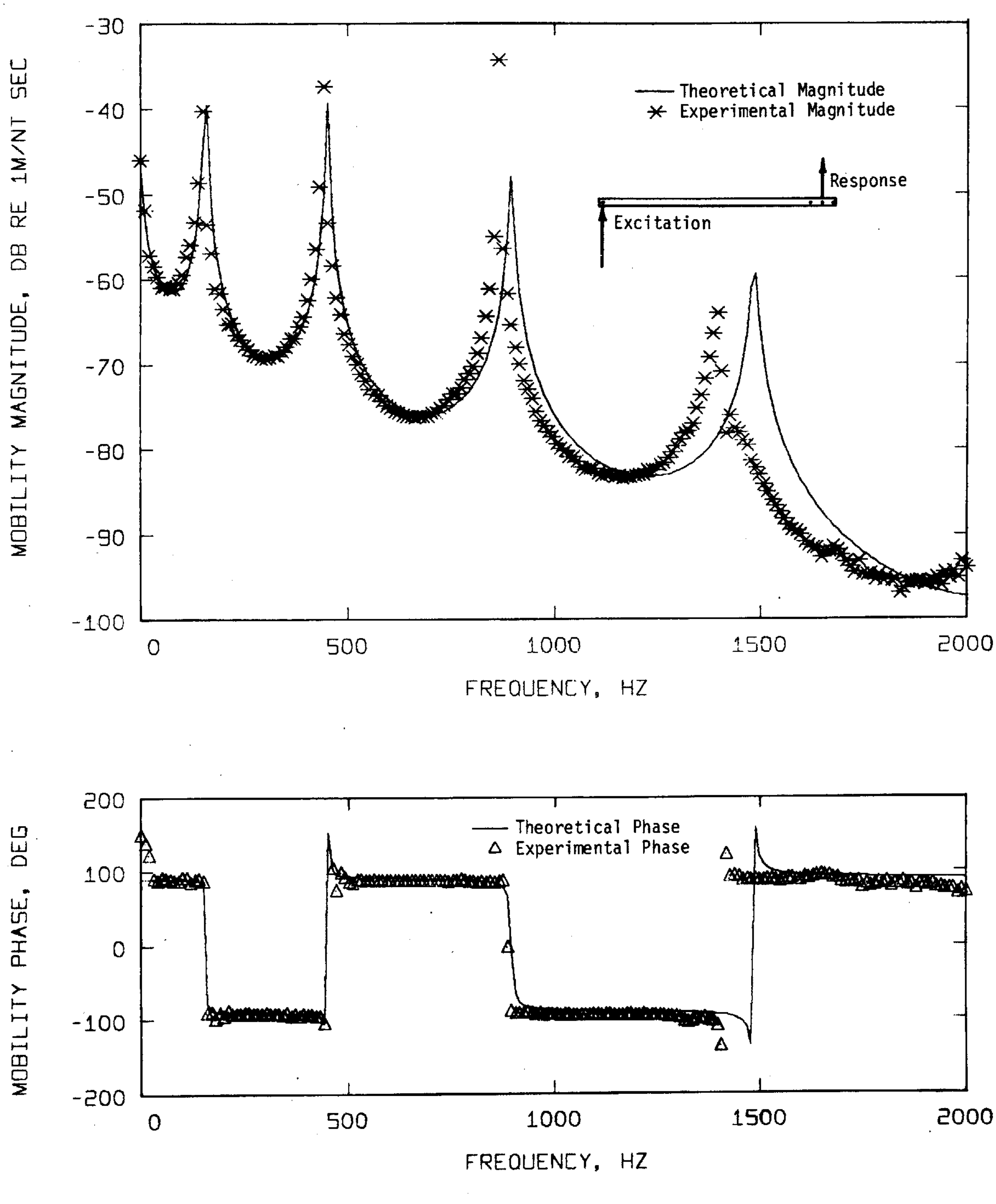

FIGURE 3.6: Test Beam Experimental and Theoretical Translational Mobility $\psi_{3,1}$

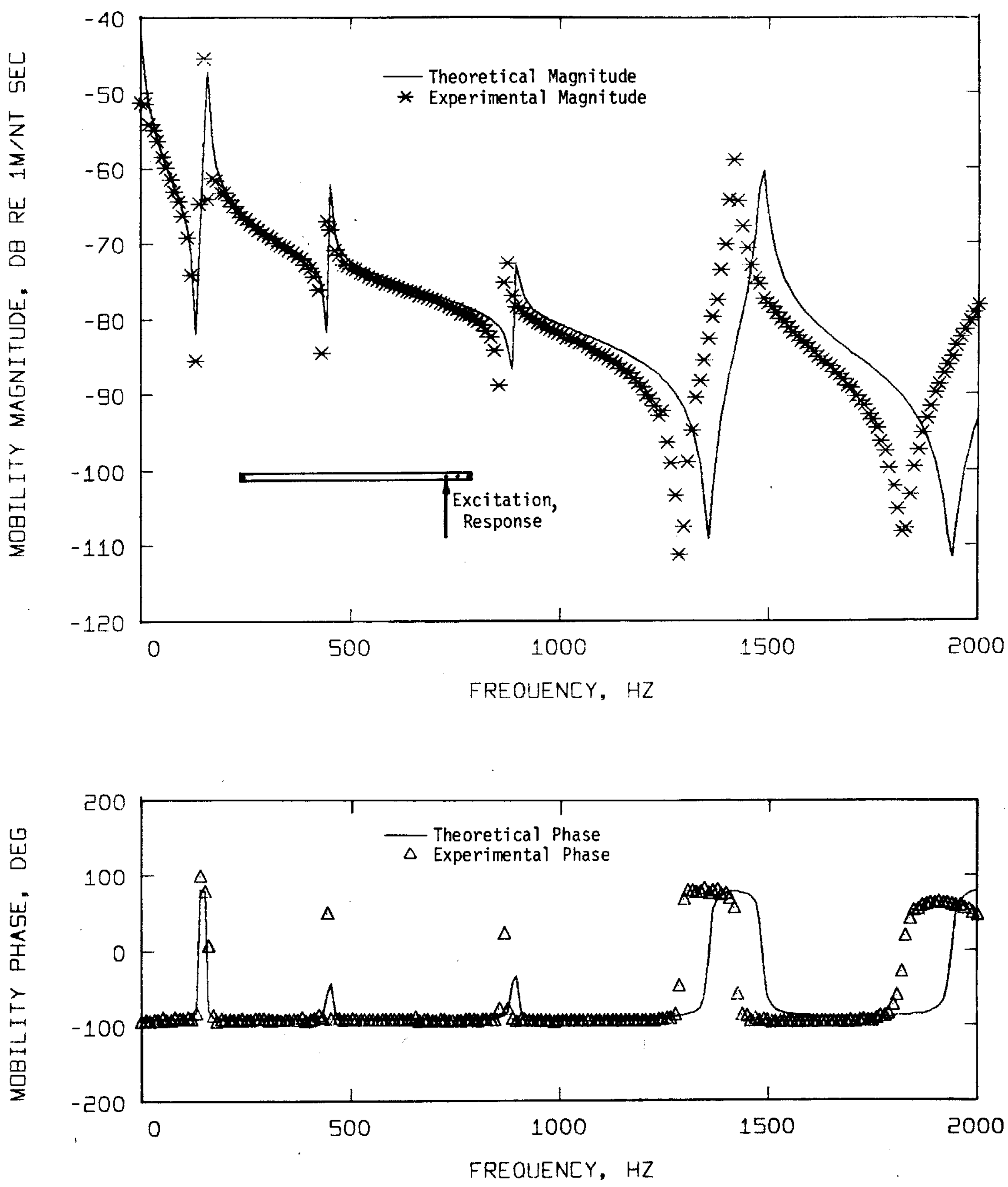

FIGURE 3.7: Test Beam Experimental and Theoretical Translational Mobility $\psi_{2,2}$

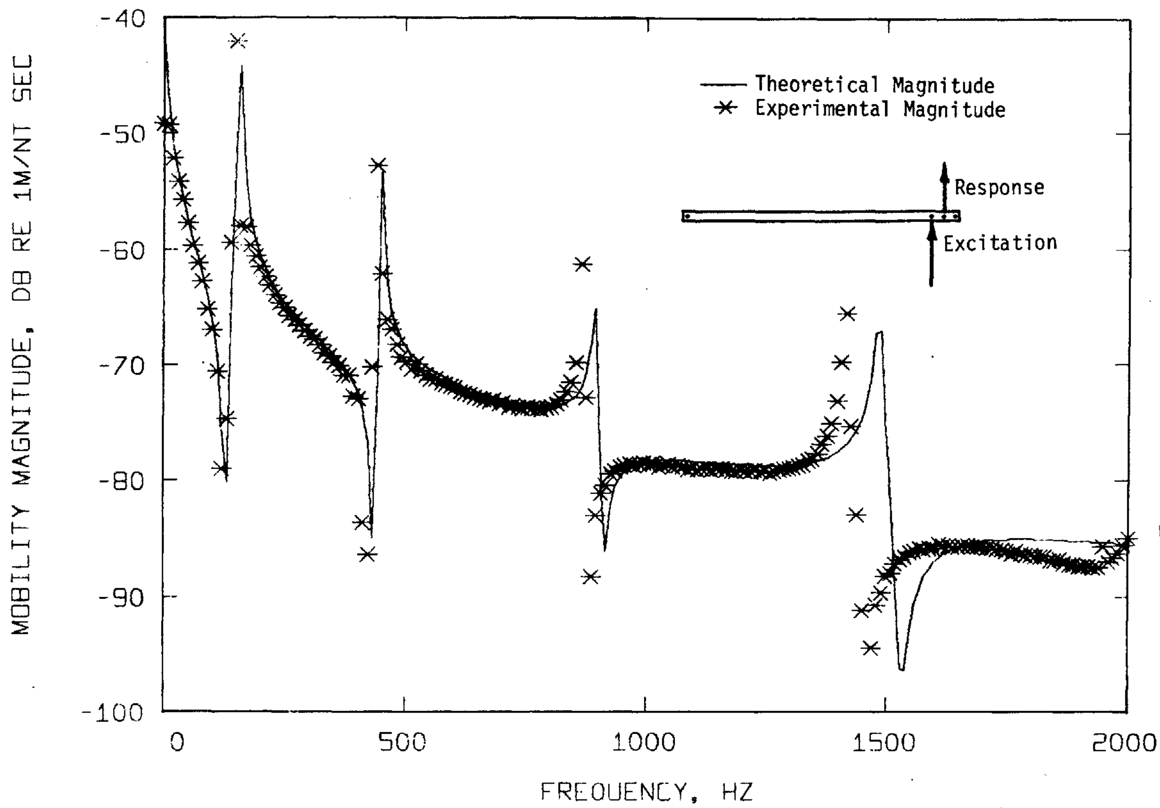

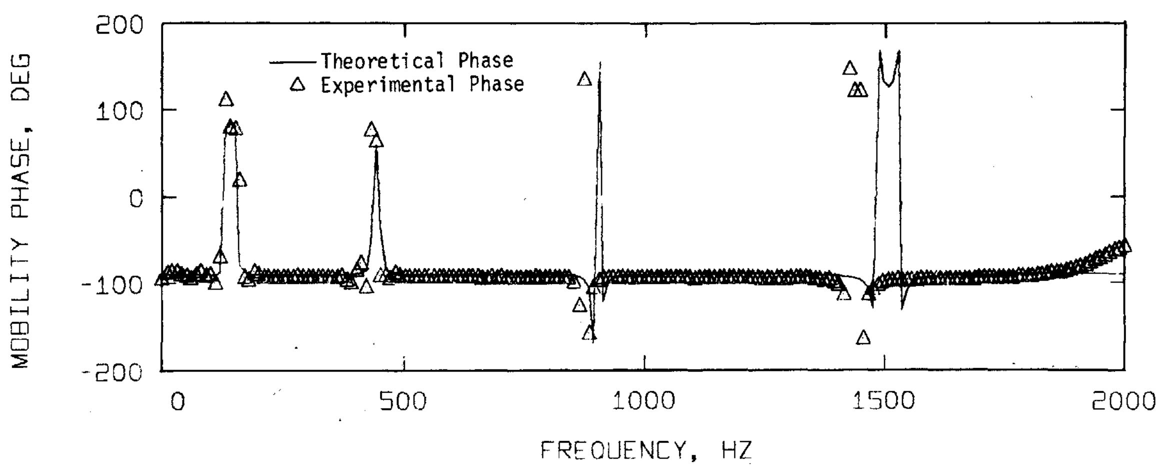

FIGURE 3.8: Test Beam Experimental and Theoretical Translational Mobility $\psi_{3,2}$

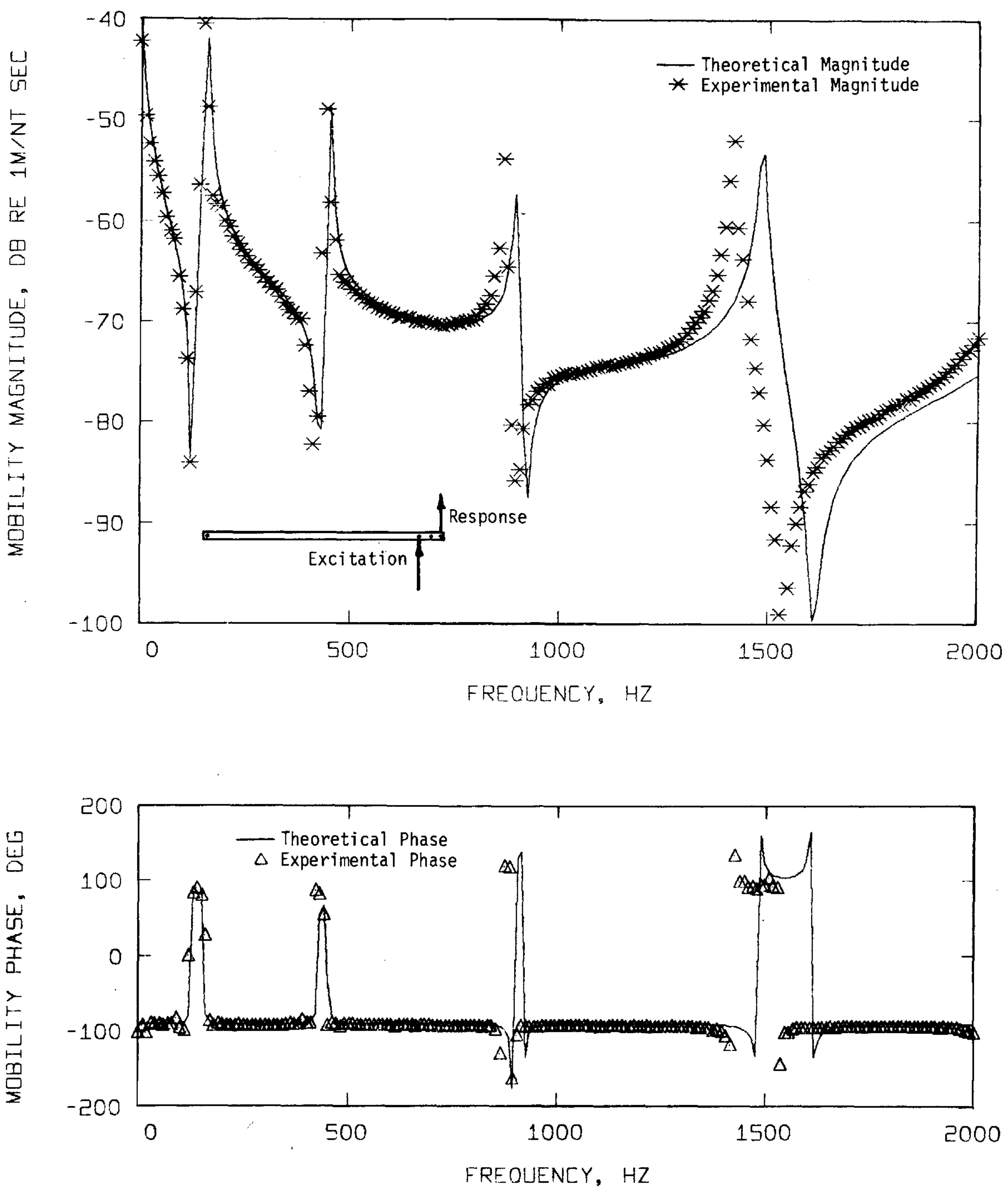

FIGURE 3.9: Test Beam Experimental and Theoretical Translational Mobility $\psi_{4,2}$

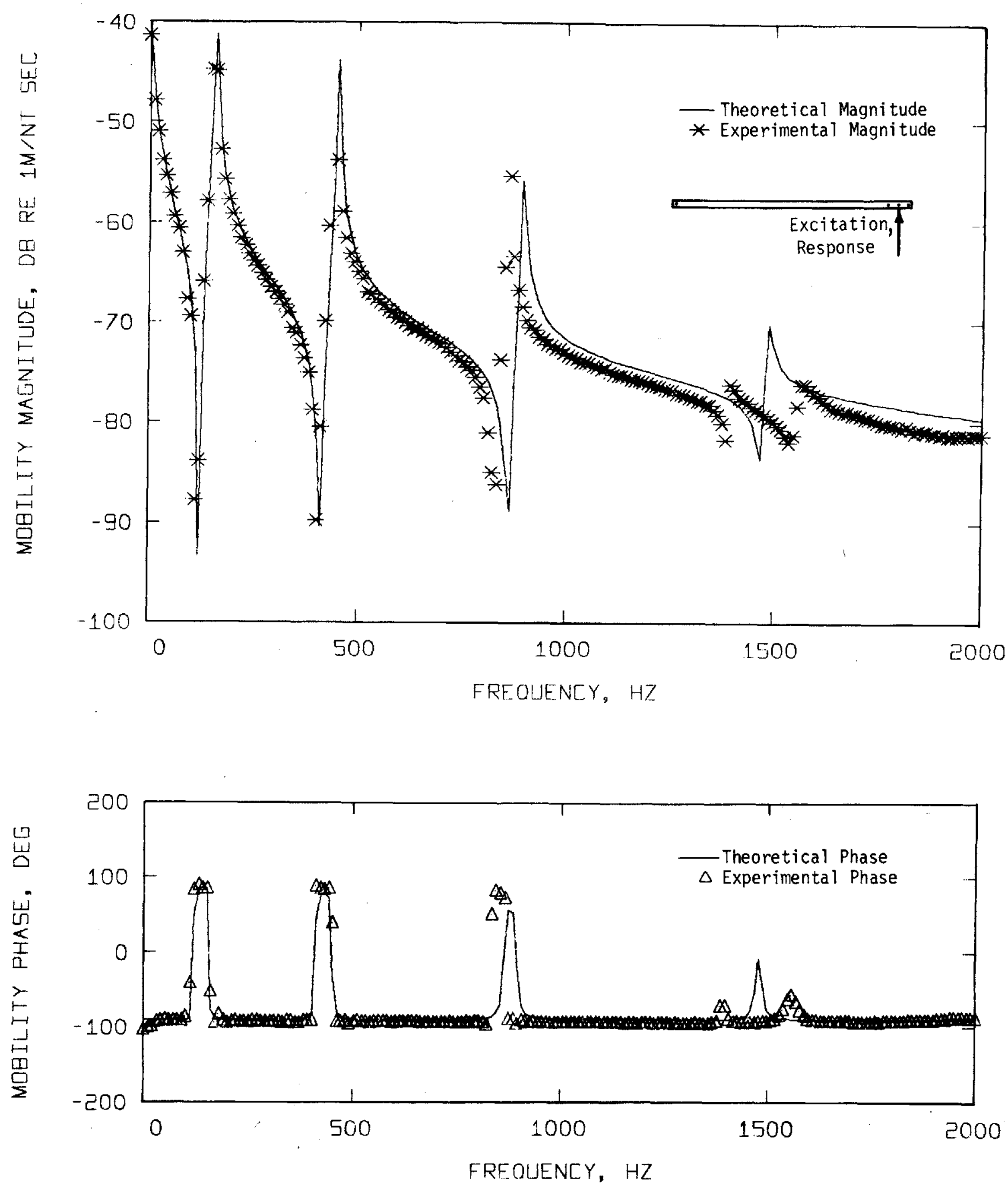

FIGURE 3.10: Test Beam Experimental and Theoretical Translational Mobility $\psi_{3,3}$

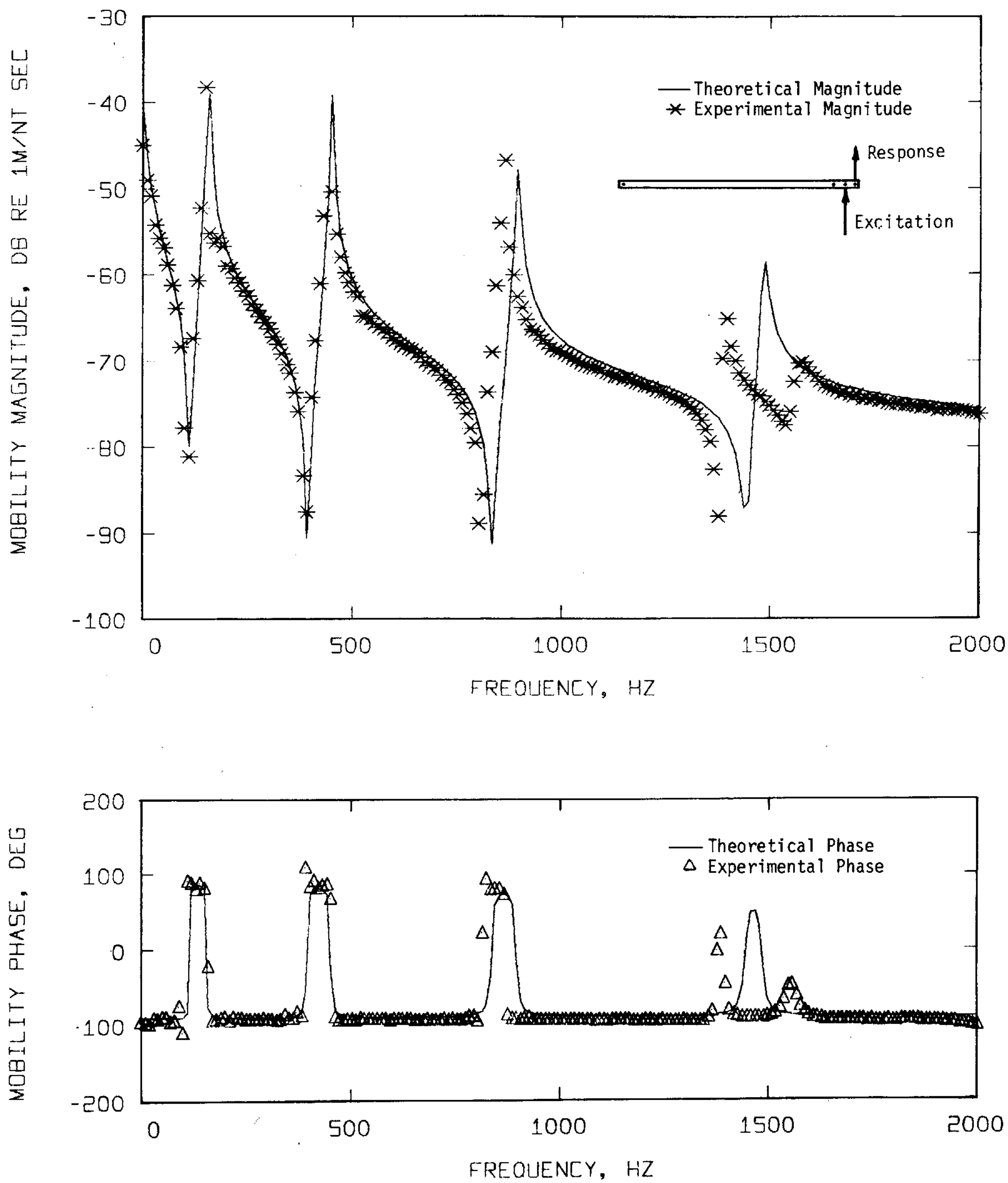

FIGURE 3.11: Test Beam Experimental and Theoretical Translational Mobility $\psi_{4,3}$

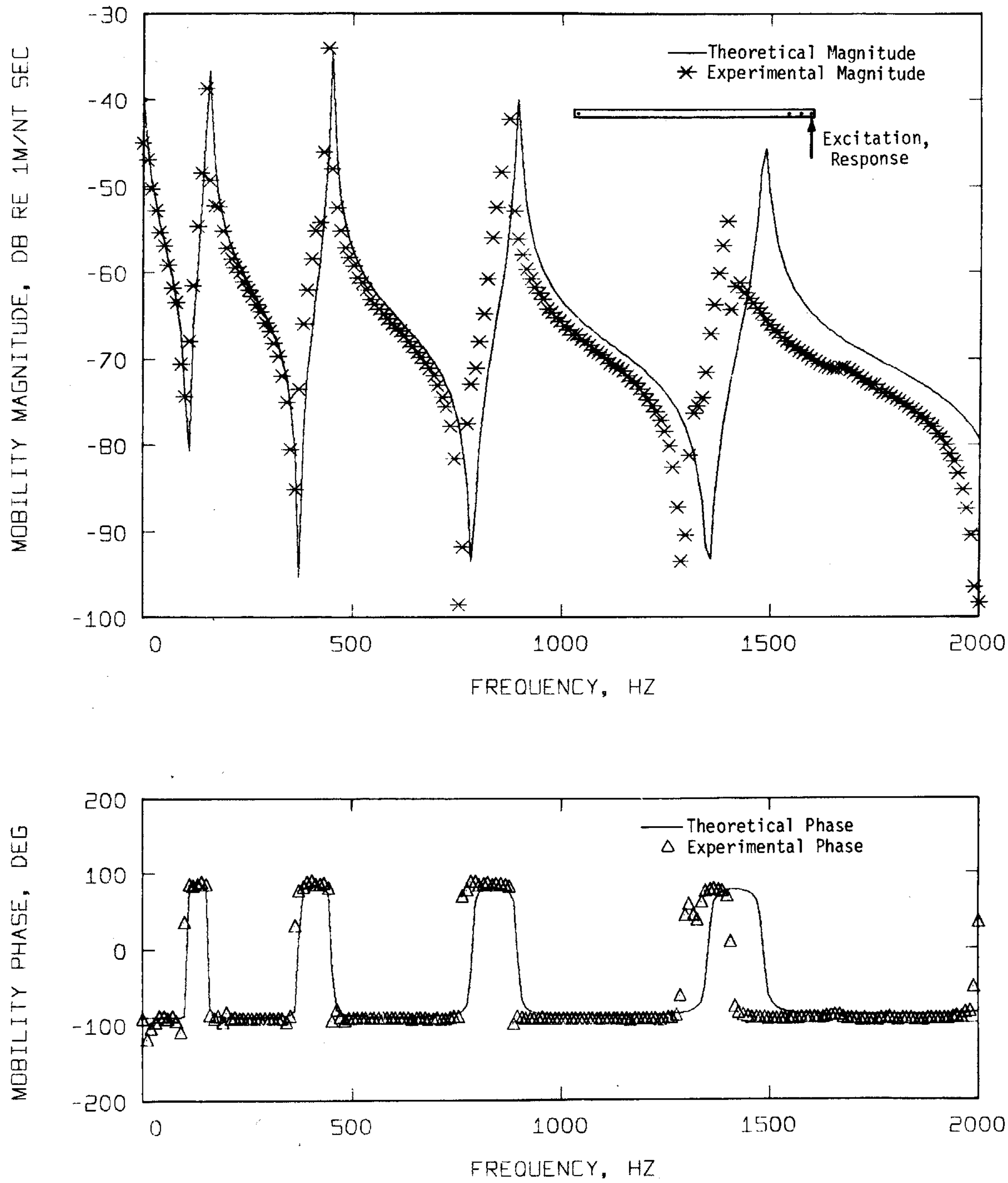

FIGURE 3.12: Test Beam Experimental and Theoretical Translational Mobility $\psi_{4,4}$

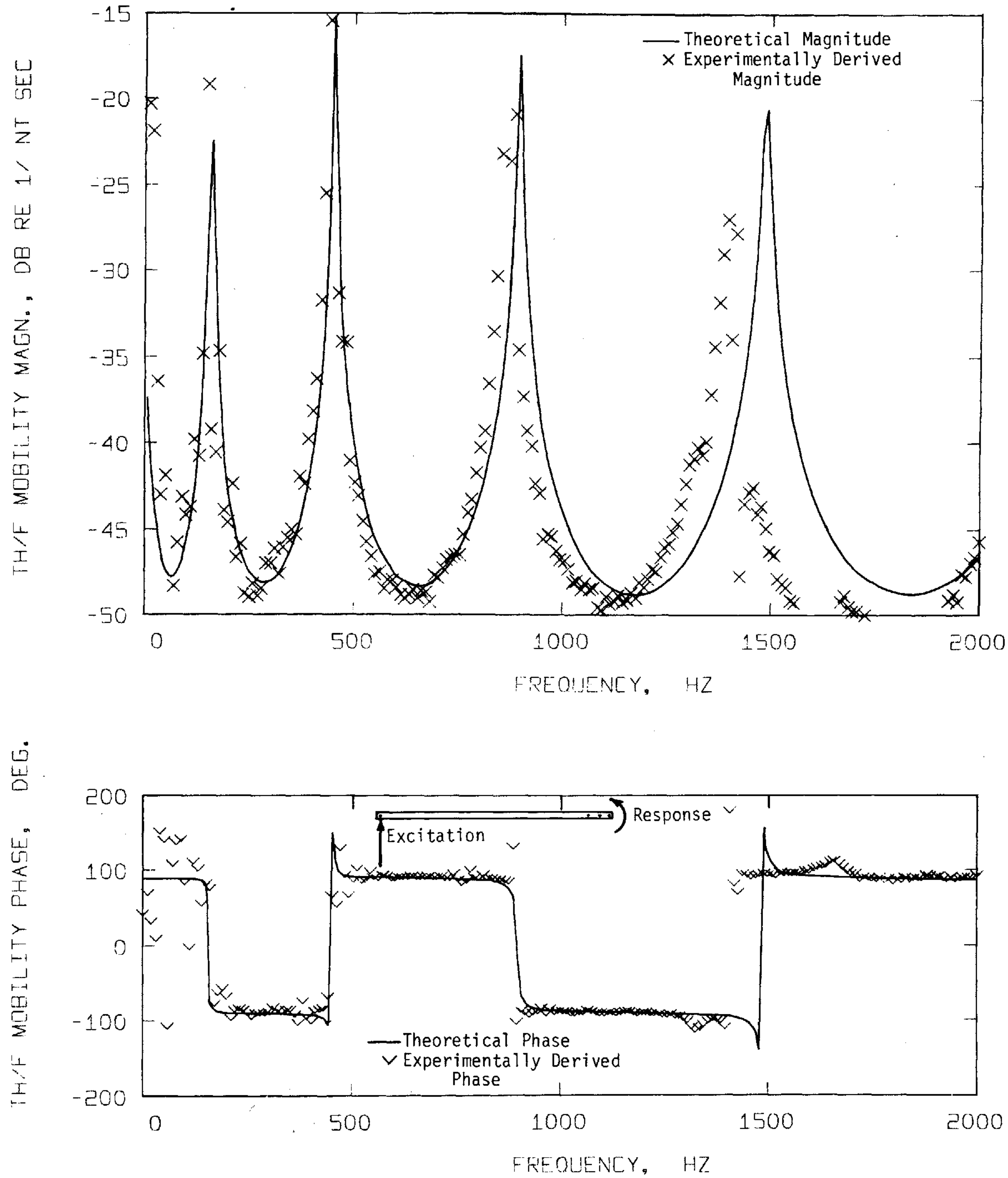

FIGURE 3.13: Test Beam Experimental and Theoretical Rotational Velocity/Force Mobility $Y_{\Theta_B F_A}(\omega)$

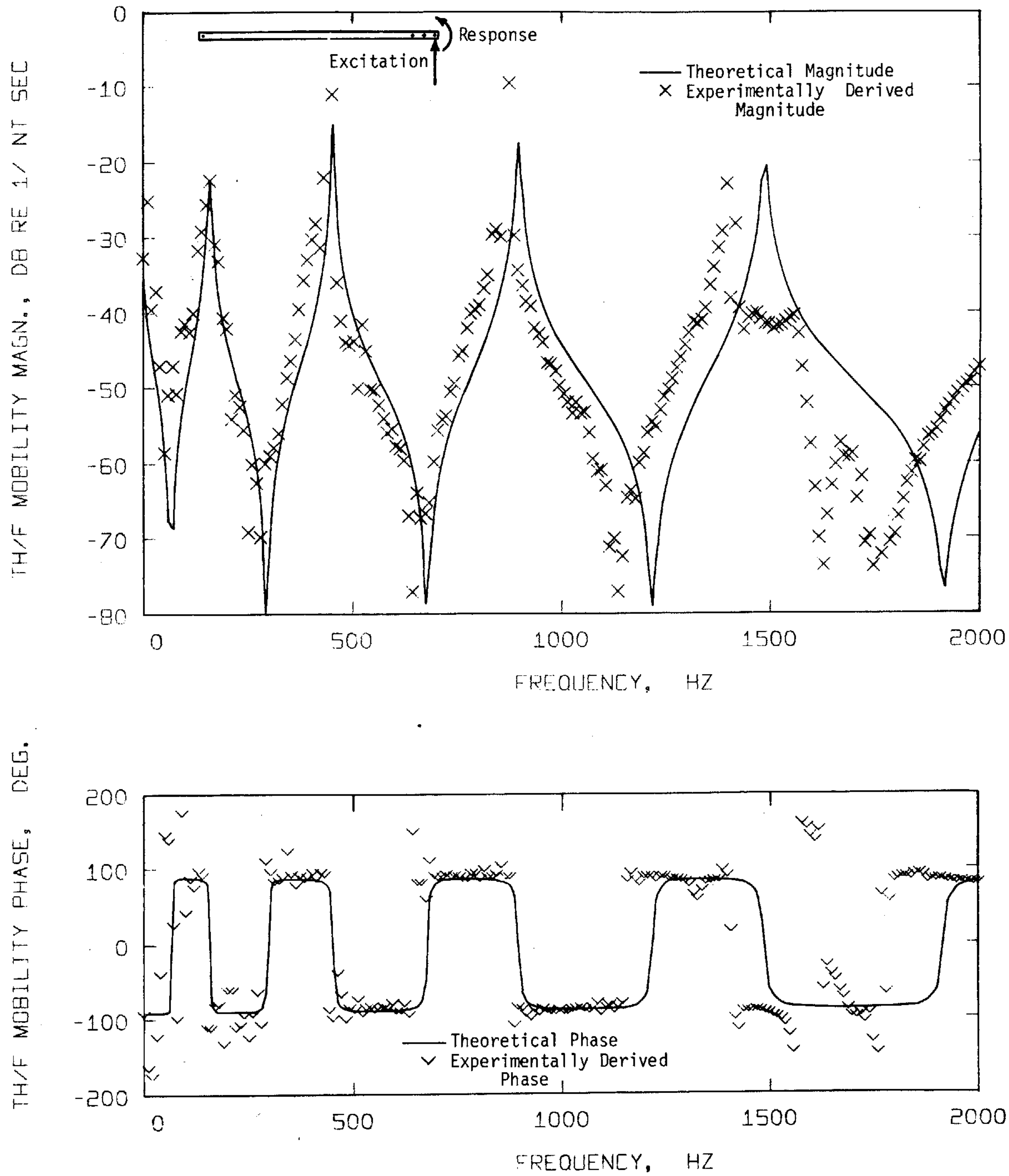

FIGURE 3.14: Test Beam Experimental and Theoretical Rotational Velocity/Force Mobility $Y_{\Theta_B F_B}(\omega)$

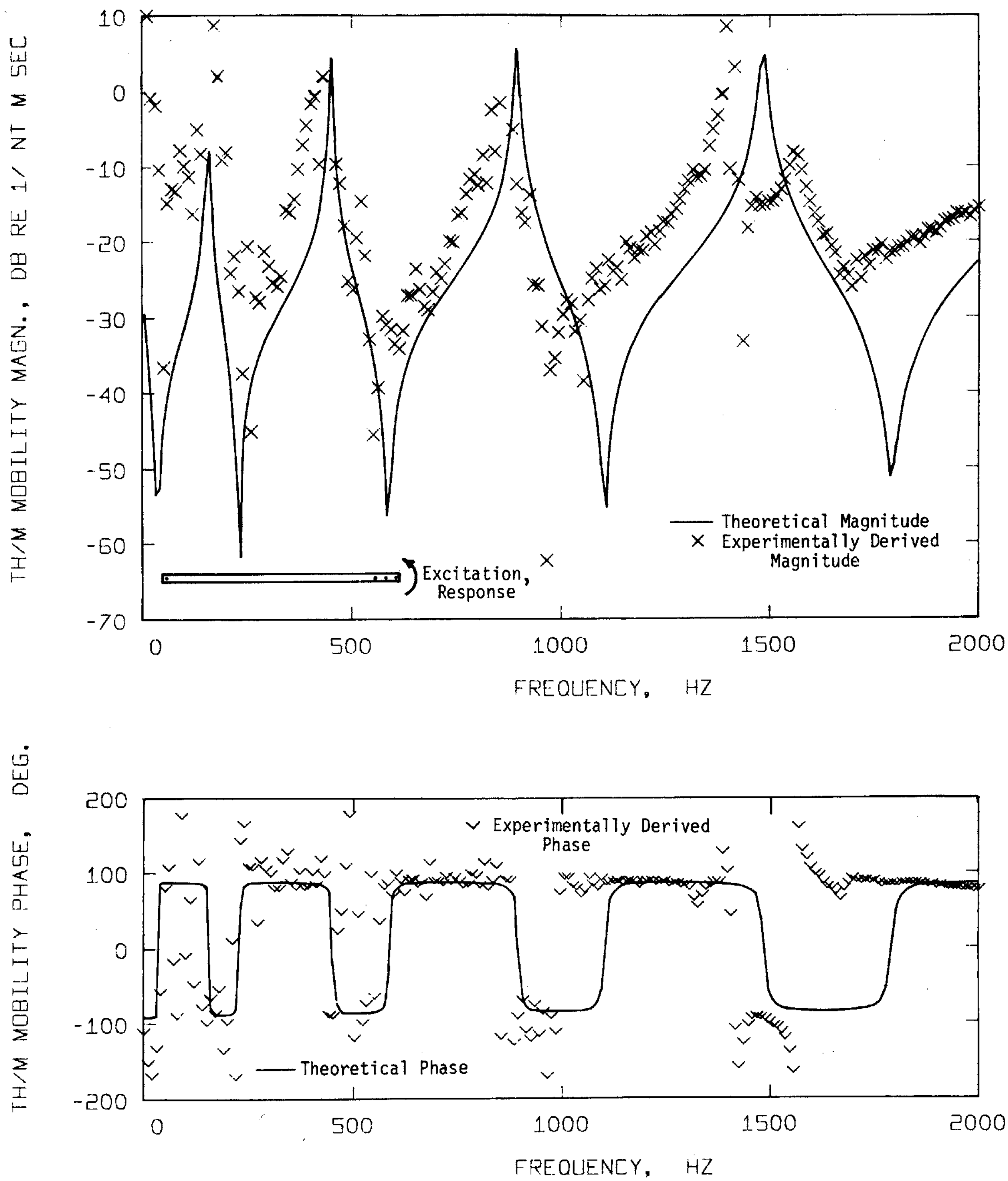

FIGURE 3.15: Test Beam Experimental and Theoretical Rotational Velocity/ Moment Mobility $Y_{\Theta_B M_B}(\omega)$

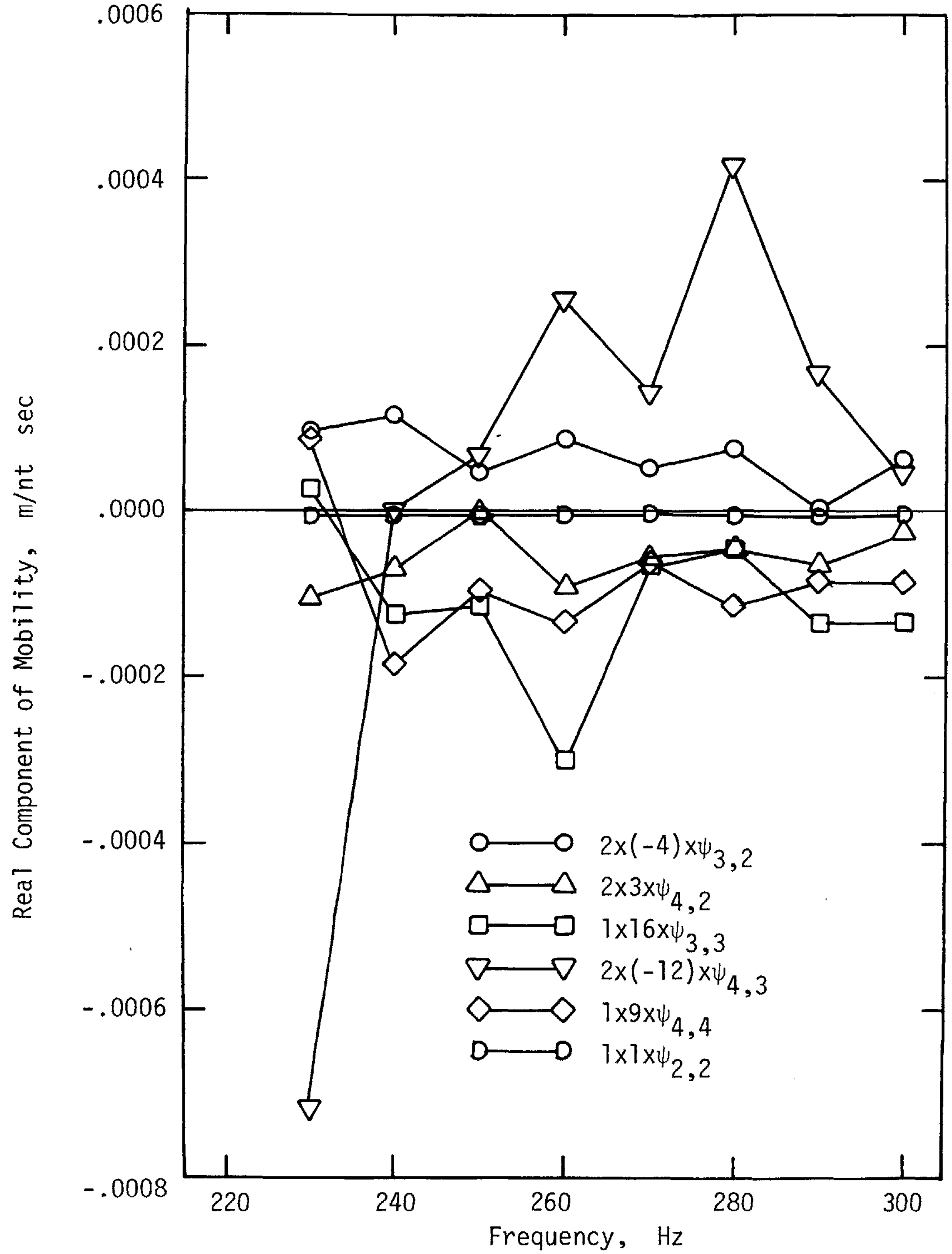

FIGURE 3.16: Constituent Terms of Derived Experimental Mobility $Y_{\theta_B M_B}(\omega)$ Over a Frequency Band of Large Scatter: Real Components

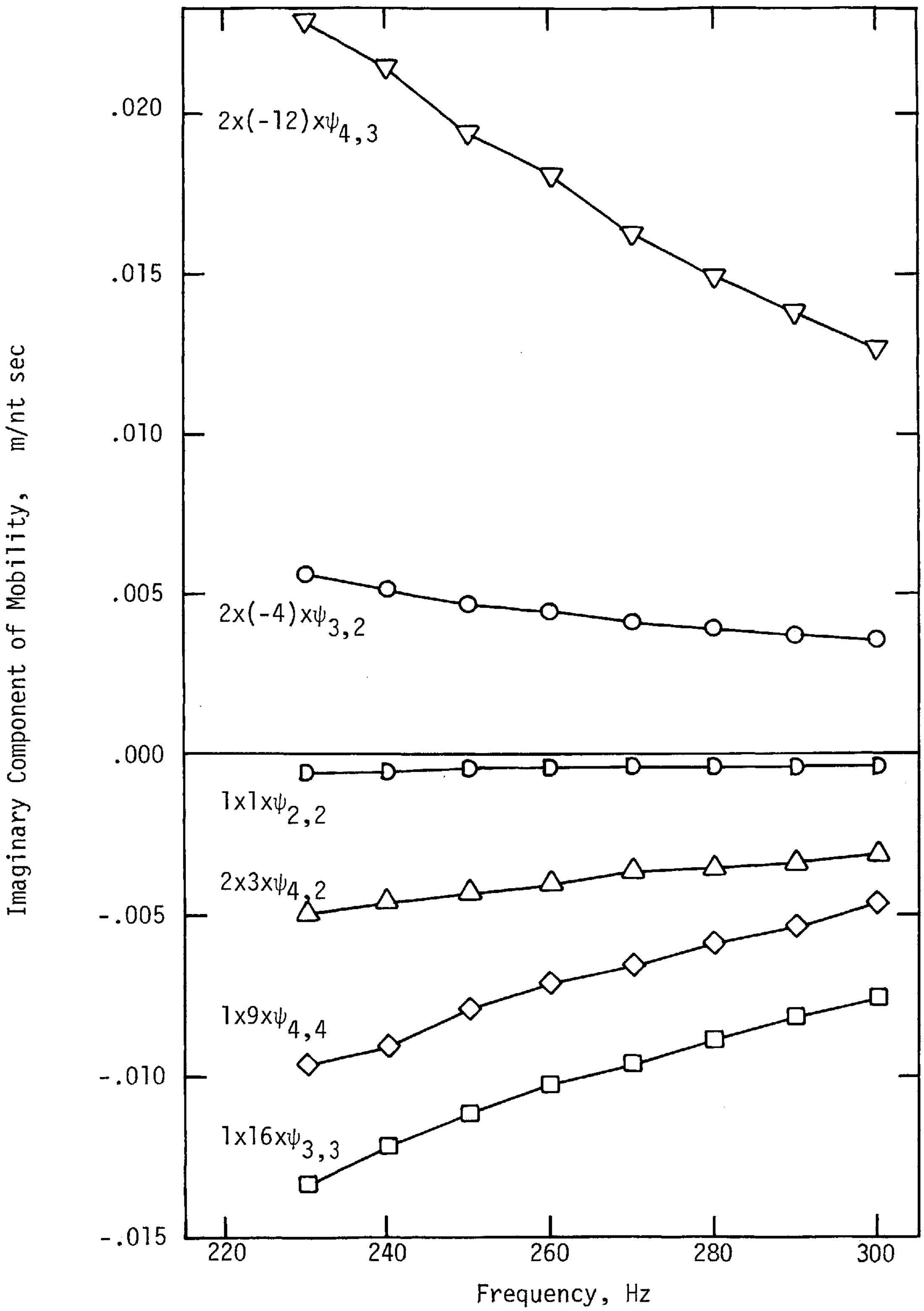

FIGURE 3.17: Constituent Terms of Derived Experimental Mobility $Y_{\Theta_B M_B}(\omega)$ Over a Frequency Band of Large Scatter: Imaginary Components

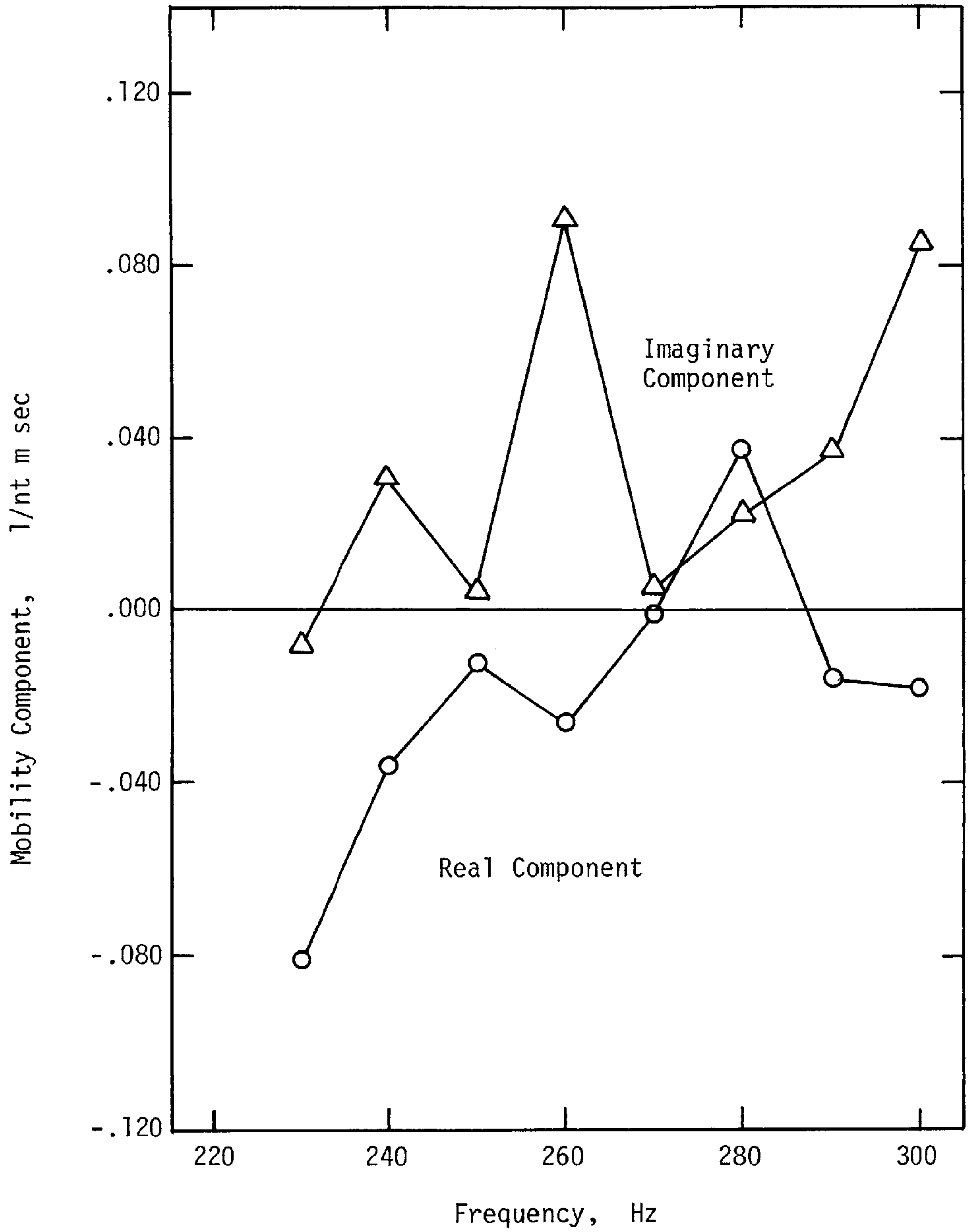

FIGURE 3.18: Quadrature Components of the Derived Experimental Mobility $Y_{\Theta_B M_B}(\omega)$ Over the Frequency Band of Figures 3.16 and 3.17

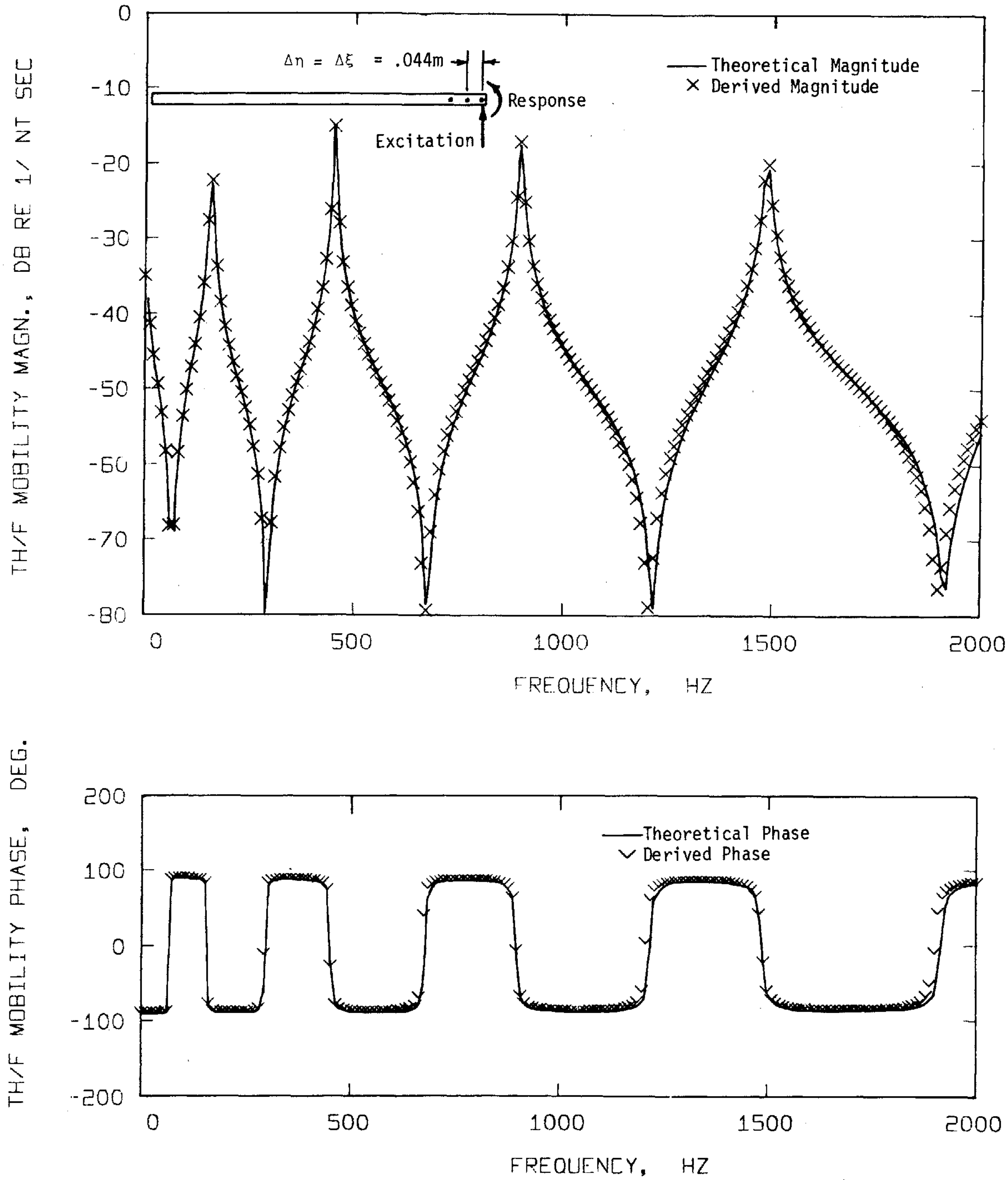

FIGURE 3.19 Rotational Velocity/Force Mobility $Y_{\Theta_B F_B}(\omega)$ Derived by Differencing Theoretical Translational Mobilities: $\Delta\eta = \Delta\xi = .044$m

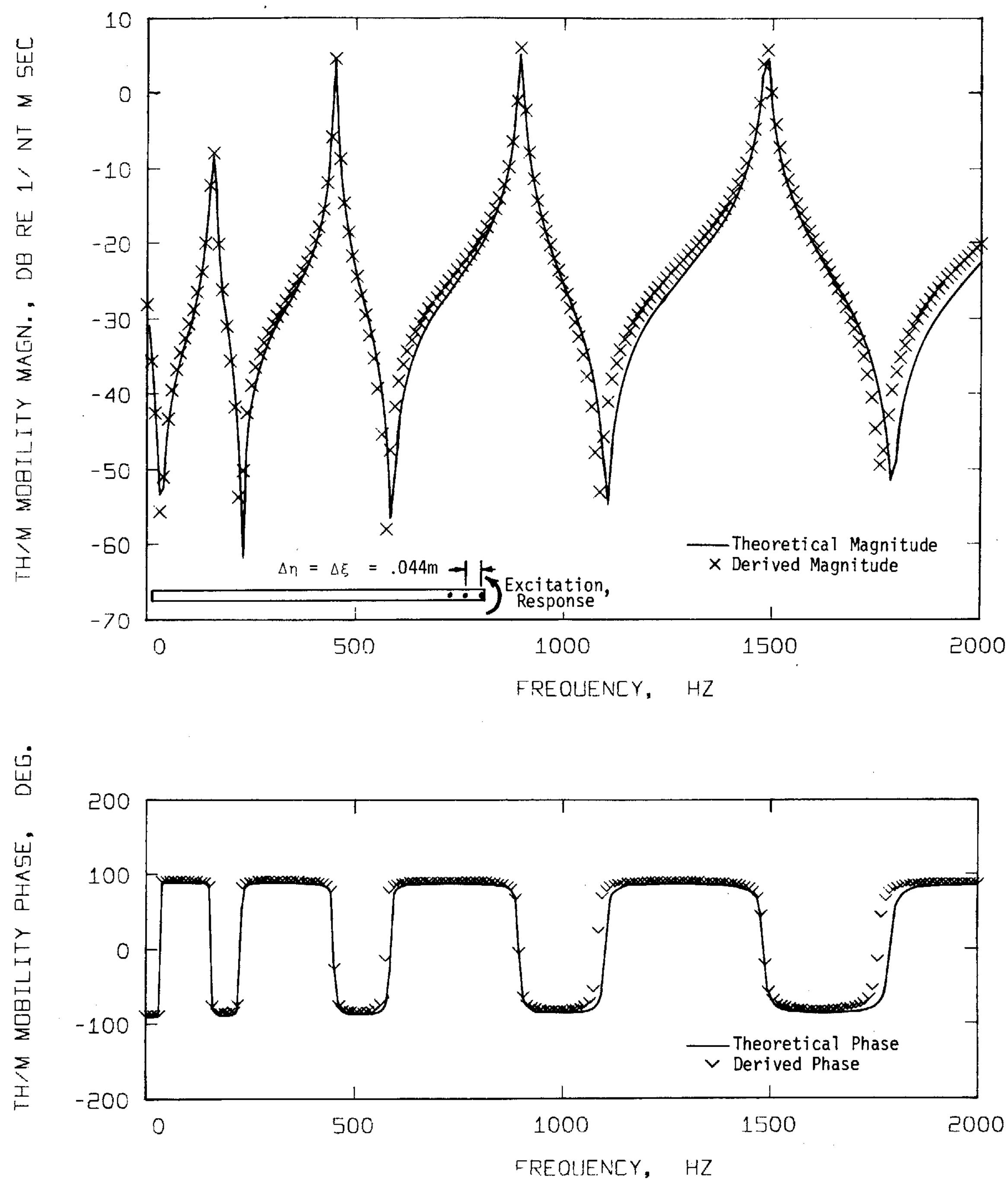

FIGURE 3:20: **Rotational Velocity/Moment Mobility $Y_{\Theta_B M_B}(\omega)$ Derived by Differencing Theoretical Translational Mobilities: $\Delta\eta = \Delta\xi = .044m$**

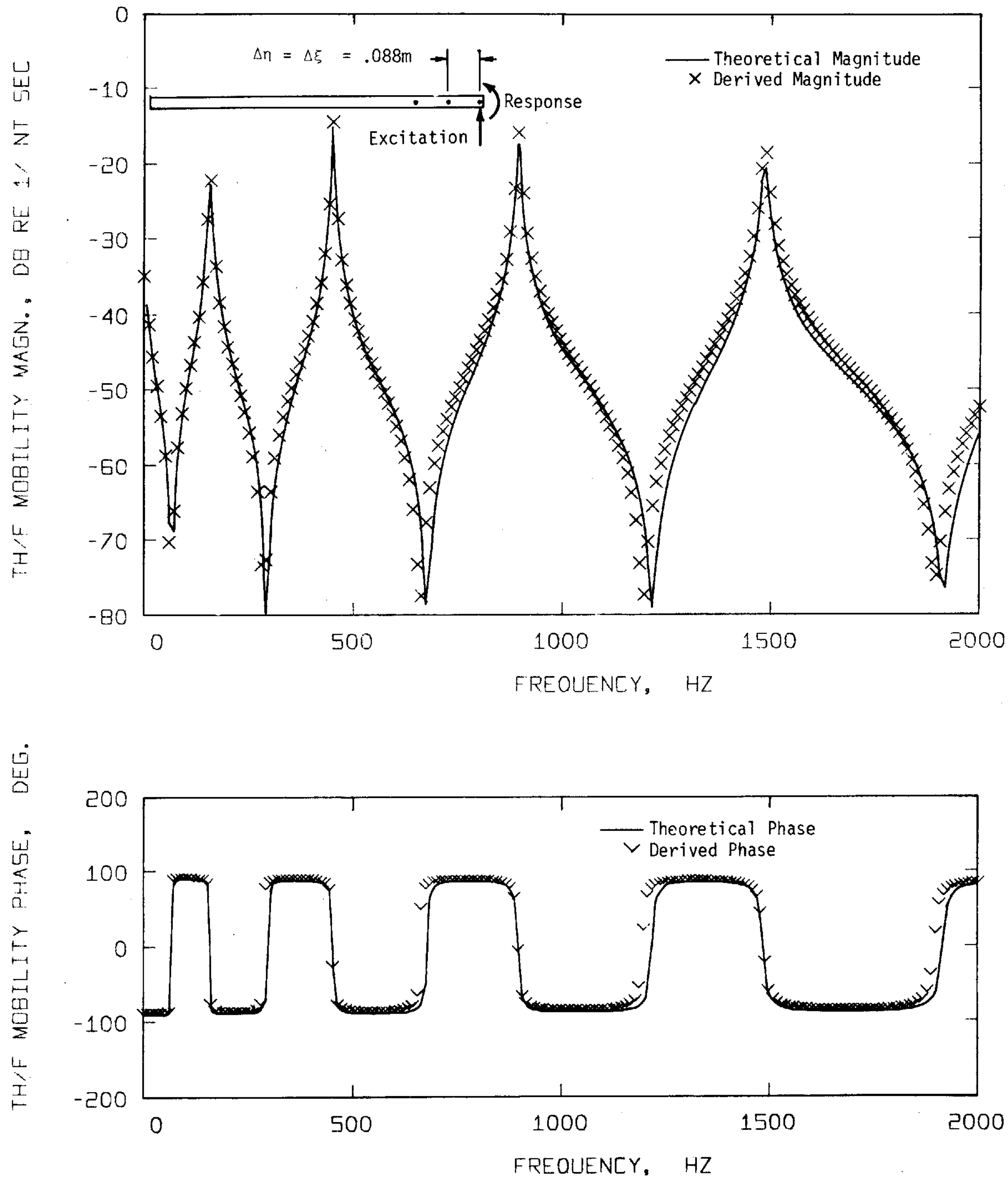

FIGURE 3.21: Rotational Velocity/Force Mobility $Y_{\theta_B F_B}(\omega)$ Derived by Differencing Theoretical Translational Mobilities:
$\Delta\eta = \Delta\xi = .088m$

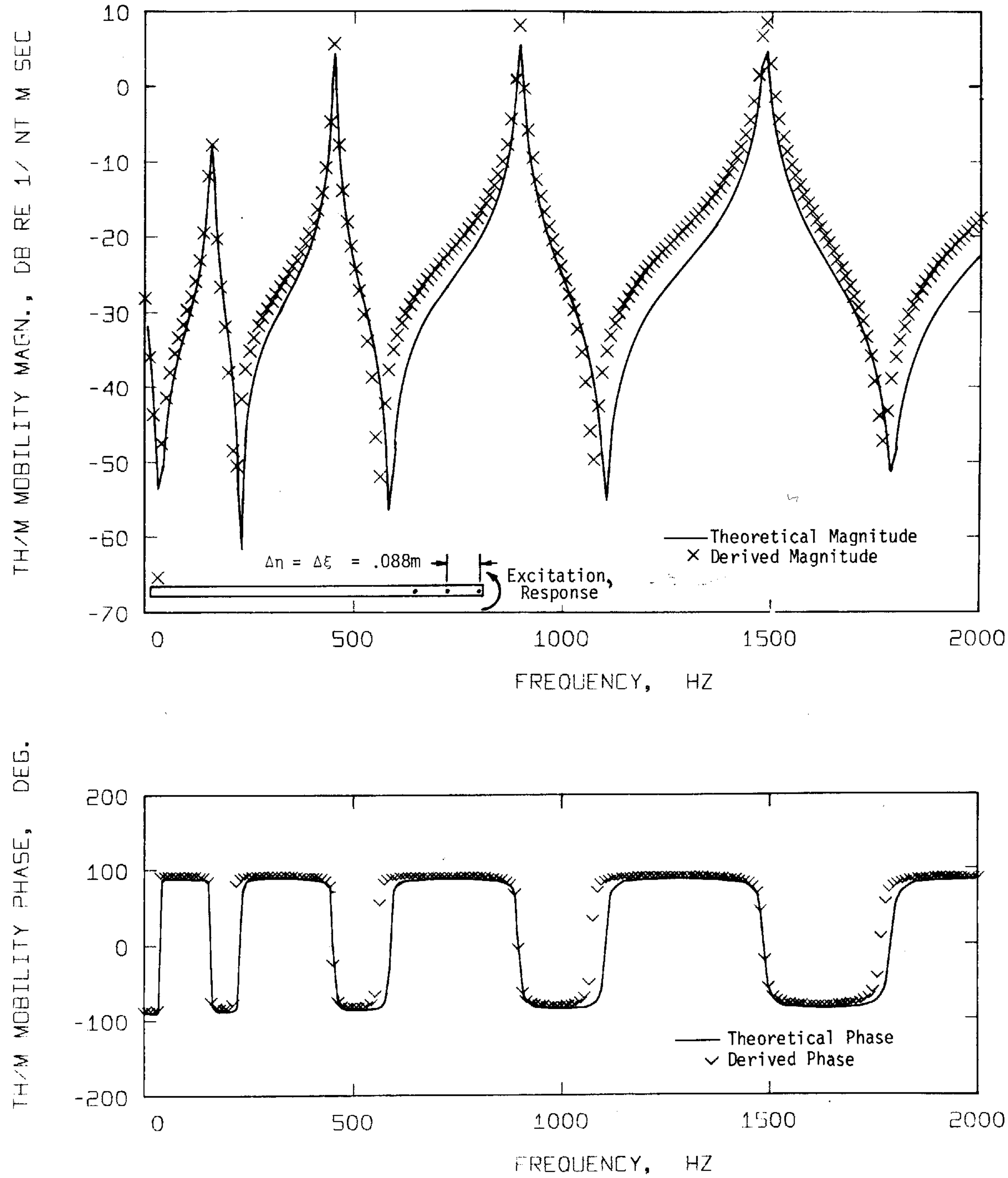

FIGURE 3.22: Rotational Velocity/Moment Mobility $Y_{\Theta_B M_B}(\omega)$ Derived by Differencing Theoretical Translational Mobilities: $\Delta\eta = \Delta\xi = .088$m

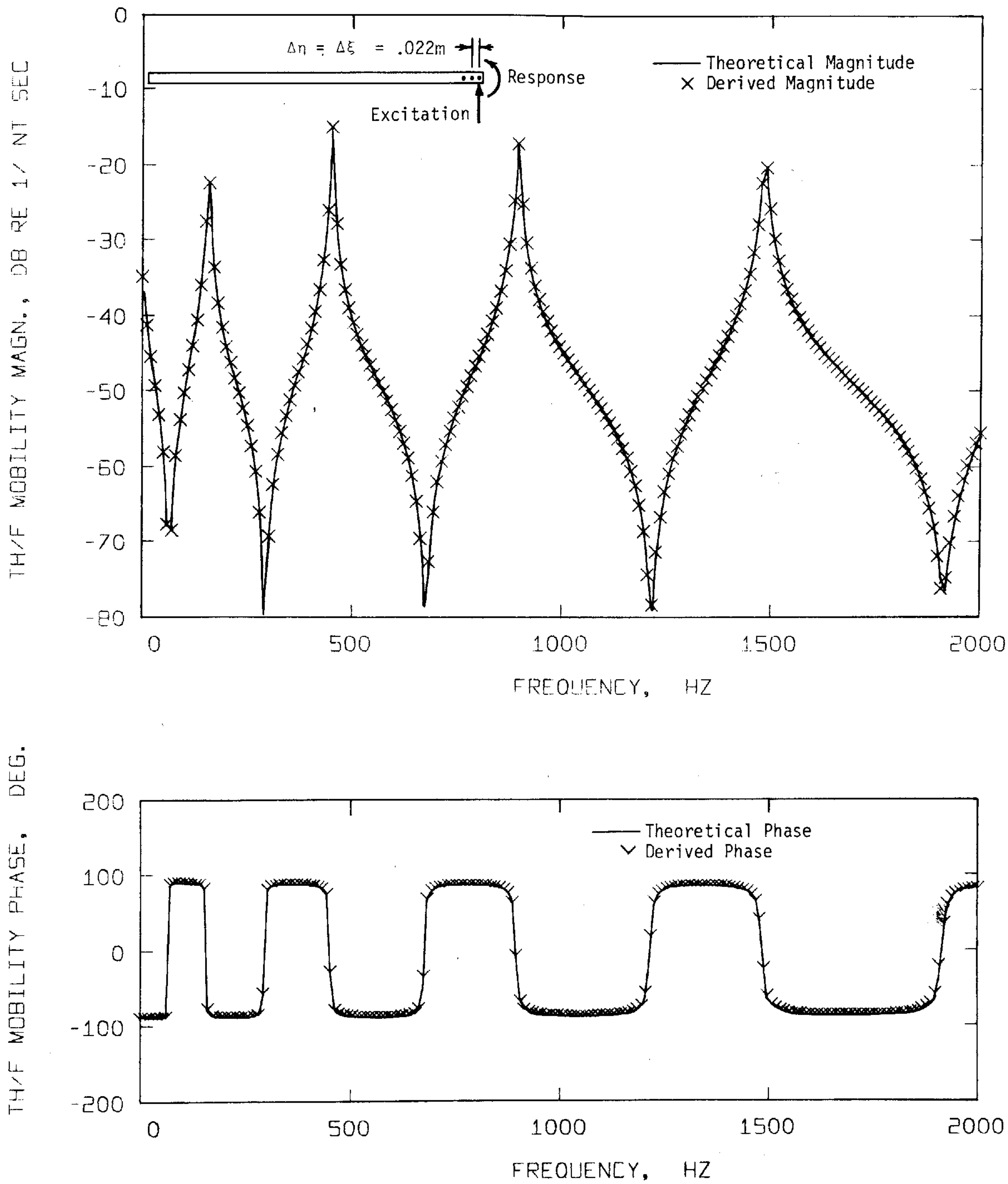

FIGURE 3.23: Rotational Velocity/Force Mobility $Y_{\Theta_B F_B}(\omega)$ Derived by Differencing Theoretical Translational Mobilities: $\Delta\eta = \Delta\xi = .022\text{m}$

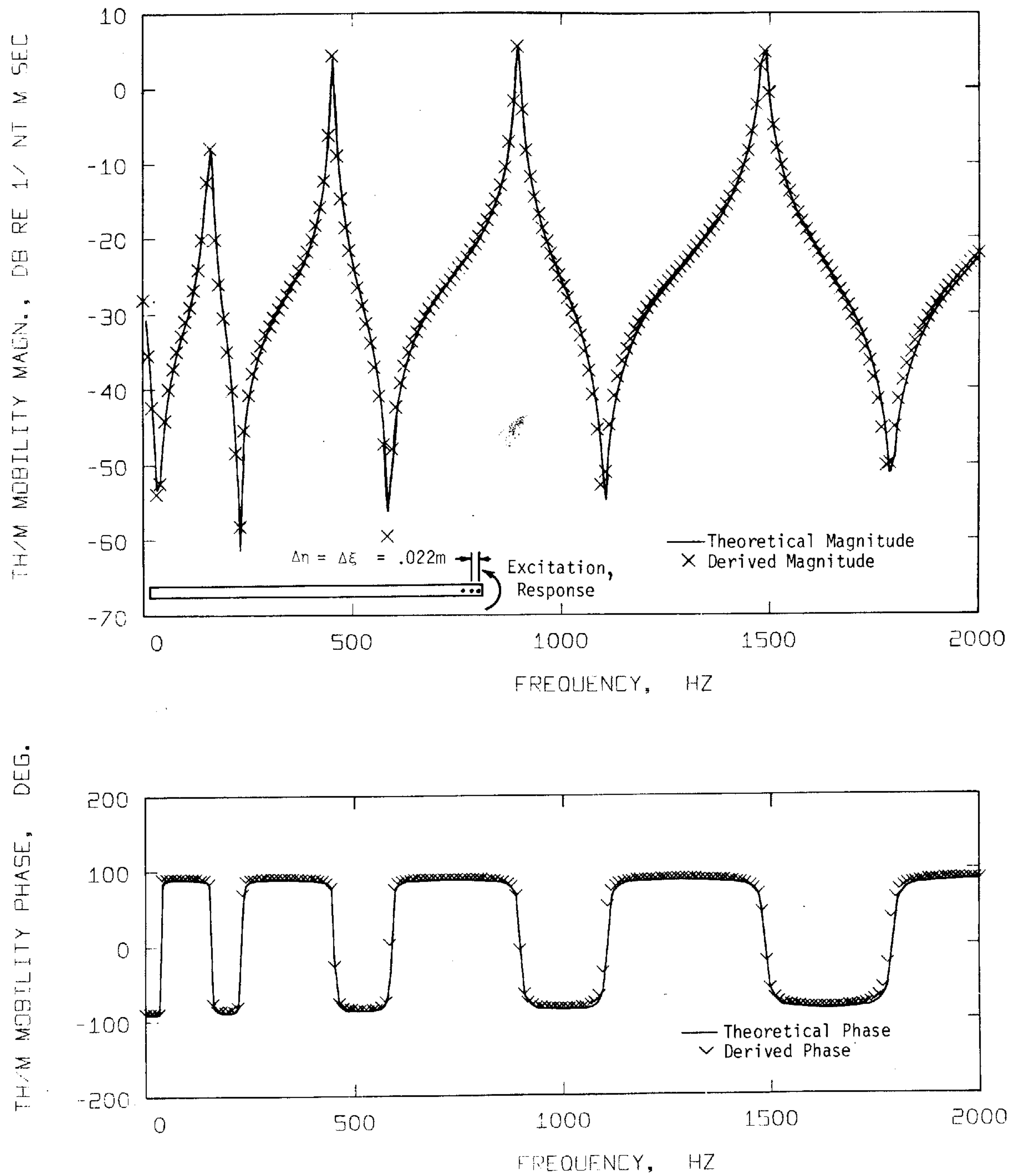

FIGURE 3.24: **Rotational Velocity/Moment Mobility $Y_{\Theta_B M_B}(\omega)$ Derived by Differencing Theoretical Translational Mobilities:** $\Delta\eta = \Delta\xi = .022m$

REFERENCES

1. W. C. Ballard, S. L. Casey, and J. D. Clausen, "Vibration Testing with Mechanical Impedance Methods," *Sound and Vibration*, January, 1969, pp 10-21.

2. J. V. Otts and C. E. Nuckolls, "A Progress Report on Force-Controlled Vibration Testing," *J. Environmental Science*, December, 1965, pp 24-28.

3. R. M. Mains, "The Application of Impedance Techniques to a Shipboard Vibration Absorber", *Shock and Vibration Bulletin, 33*, 4, March, 1964.

4. A. L. Klosterman and J. R. Lemon, "Dynamic Design Analysis Via the Building Block Approach", *Shock and Vibration Bulletin, 42*, 1, January, 1972.

5. R. DeJong, "Vibration Energy Transfer in a Diesel Engine", ScD Thesis, MIT, Dept. of Mech. Eng., 1976.

6. D. U. Noiseux and E. B. Meyer, "Application of Impedance Theory and Measurements to Structural Vibration, U.S. Air Force Flight Dynamics Laboratory Tech. Rept. AFFDL-TR-67-182.

7. F. J. On, "Preliminary Study of an Experimental Method in Multidimensional Mechanical Impedance Determination", *Shock and Vibration Bulletin, 34*, 3, December, 1964.

8. J. E. Smith, "Measurement of the Total Structural Mobility Matrix," *Shock and Vibration Bulletin, 40*, 7, December, 1969.

9. D. J. Ewins and P. T. Gleeson, "Experimental Determination of Multidirectional Mobility Data for Beams", *Shock and Vibration Bulletin, 45*, 5, June, 1975.

10. E. Isaacson and H. B. Keller, *Analysis of Numerical Methods*, John Wiley & Sons, Inc., New York, 1966.

11. J. W. Leech, L. Morino, and E. A. Witmer, "PETROS 2: A New Finite-Difference Method and Program for the Calculation of Large Elastic-Plastic Dynamically-Induced Deformations of General Thin Shells," U. S. Army Ballistic Research Laboratories, ASRL TR152, Contract Report No. 12, December, 1969.

12. S. Timoshenko, D. H. Young and W. Weaver, Jr., *Vibration Problems in Engineering,* 4th Ed., John Wiley & Sons, Inc., New York, 1974.

13. L. Meirovitch, *Analytical Methods in Vibrations,* Macmillan Company, 1967.

14. R. D. Cavanaugh and J. E. Ruzicka, "Vibration Isolation of Non-Rigid Bodies", Colloquium on Mechanical Impedance Methods, ASME, New York,1958.

APPENDIX A

THEORETICAL MOBILITIES OF A FREE-FREE BEAM

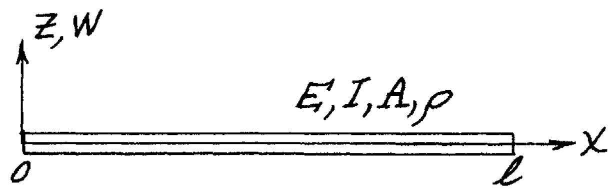

The governing partial differential equation for the free vibration of an undamped uniform beam is given by Eq. (5.82) of Ref. (12) as

$$EI \frac{\partial^4 w}{\partial x^4} = -\rho A \frac{\partial^2 w}{\partial t^2} \quad . \tag{A.1}$$

The derivation of this equation, referred to as the Bernoulli-Euler beam equation, is based on the assumption that the effects of rotary inertia and shearing deformations are negligible in comparison with the effects of translational inertia and flexural deformations (i.e., the beam is slender).

The free vibration mode shapes and frequencies are obtained by first assuming a harmonic solution of the form

$$w(x,t) = W(x)\, e^{i\omega t} \quad . \tag{A.2}$$

Substitution of this expression into Eq.(A.1) results in the ordinary differential equation

$$EIW'''' - \rho A \omega^2 W = 0 \tag{A.3}$$

where the prime notation indicates differentiation with respect to x. Setting

$$p^4 = \frac{\rho A \omega^2}{EI} \quad , \tag{A.4}$$

the general solution of Eq. (4.3) can be written

$$W(x) = C_1 \sinh px + C_2 \cosh px + C_3 \sin px + C_4 \cos px \tag{A.5}$$

for which the first three derivatives are:

$$W'(x) = pC_1 \cosh px + pC_2 \sinh px + pC_3 \cos px - pC_4 \sin px$$

$$W''(x) = p^2 C_1 \sinh px + p^2 C_2 \cosh px - p^2 C_3 \sin px - p^2 C_4 \cos px \tag{A.6}$$

$$W'''(x) = p^3 C_1 \cosh px + p^3 C_2 \sinh px - p^3 C_3 \cos px + p^3 C_4 \sin px .$$

The boundary conditions for a free-free beam are as follows:

$$x=0\begin{cases}EI\dfrac{\partial^2 w}{\partial x^2}=0\\ EI\dfrac{\partial^3 w}{\partial x^3}=0\end{cases}\qquad x=\ell\begin{cases}EI\dfrac{\partial^2 w}{\partial x^2}=0\\ EI\dfrac{\partial^3 w}{\partial x^3}=0\end{cases}\tag{A.7}$$

or, simplifying slightly,

$$\begin{aligned}W''(0)&=0 \qquad & W''(\ell)&=0\\ W'''(0)&=0 \qquad & W'''(\ell)&=0 \quad .\end{aligned}\tag{A.8}$$

Inserting the Eq. (A.8) boundary conditions into Eq. (A.5) and (A.6) gives the system of equations

$$\begin{bmatrix}0 & 1 & 0 & -1\\ 1 & 0 & -1 & 0\\ \sinh p\ell & \cosh p\ell & -\sin p\ell & -\cos p\ell\\ \cosh p\ell & \sinh p\ell & -\cos p\ell & \sin p\ell\end{bmatrix}\begin{Bmatrix}C_1\\ C_2\\ C_3\\ C_4\end{Bmatrix}=\begin{Bmatrix}0\\ 0\\ 0\\ 0\end{Bmatrix}\tag{A.9}$$

For nontrivial results, the determinant of the above 4 x 4 matrix must be equal to zero; effecting this condition yields the characteristic equation

$$\cos p\ell \cosh p\ell = 1 \quad .\tag{A.10}$$

The roots of this characteristic equation are the eigenvalues of the problem and are given in p. 165 of Ref. (13) as follows:

$$p_0 l = p_1 l = 0 \qquad \text{(rigid body modes)}$$
$$p_2 l = 4.730 \qquad \text{(first elastic mode)}$$
$$p_3 l = 7.853 \qquad \text{(second elastic mode)} \qquad \text{(A.11)}$$
$$p_r l = (2r-1)\frac{\pi}{2}, \qquad r \geq 4$$

The natural frequencies are given by:

$$\omega_r^2 = \frac{EIp_r^4}{\rho A} = \frac{EI(p_r l)^4}{\rho A l^4}$$

or

$$\omega_r = (p_r l)^2 \sqrt{\frac{EI}{\rho A l^4}} \quad . \qquad \text{(A.12)}$$

The eigenfunctions are found by arbitrarily setting $C_4 = 1$ and using the first two of Eqs. (A.9) to determine that $C_2 = 1$ and $C_1 - C_3 = 0$. When these results are inserted into the third of Eq. (A.9) it is determined that:

$$C_1 = C_3 = \frac{\cos pl - \cosh pl}{\sinh pl - \sin pl} \quad .$$

Then, the rth eigenfunction of the problem is:

$$W_r(x) = D_r\Big[\cosh p_r x + \cos p_r x - \left(\frac{\cosh p_r l - \cos p_r l}{\sinh p_r l - \sin p_r l}\right)(\sinh p_r x + \sin p_r x)\Big] \qquad \text{(A.13)}$$

for each eigenvalue $p_r, r=2,3,\ldots$, where D_r is an arbitrary multiplier. For the special case of the rigid body modes ($p_0=p_1=0$), the eigenfunctions are:

$$\begin{aligned} W_0(x) &= D_0 && \text{(rigid body translation)} \\ W_1(x) &= D_1\left(x-\frac{\ell}{2}\right) && \text{(rigid body rotation).} \end{aligned} \tag{A.14}$$

Let $\phi_r(x)$ denote the bracketed quantity in Eq. (A.13) for modes $r=2,3,\ldots$. Per Appendix B of Ref.(14) the functions $\phi_r(x)$ have the orthogonality properties

$$\begin{aligned} &\int_0^\ell \phi_n(x)\phi_m(x)\,dx = 0, \quad m \neq n \; ; \\ &\int_0^\ell \phi_n^2(x)\,dx = \ell \quad . \end{aligned} \tag{A.15}$$

Also, per p. 164 of Ref.(13), the functions $\phi_0 = 1$ and $\phi_1 = x-\frac{\ell}{2}$ are orthogonal to each other and to the functions $\phi_r(x)$; these functions also have the properties

$$\begin{aligned} &\int_0^\ell \phi_0^2(x)\,dx = \ell \quad ; \\ &\int_0^\ell \phi_1^2(x)\,dx = \frac{\ell^3}{12} \quad . \end{aligned} \tag{A.16}$$

At this point the forced vibration response for the undamped beam can be evaluated in terms of the preceding eigenfunctions.

Let

$$w(x,t) = \sum_{r=0}^{\infty} \phi_r(x) q_r(t) \tag{A.17}$$

where the $q_r(t)$ quantities are time-varying generalized coordinates to be determined. Placing this expression into the governing partial differential equation with forcing term,

$$EI \frac{\partial^4 w}{\partial x^4} + \rho A \frac{\partial^2 w}{\partial t^2} = f(x,t) \quad , \tag{A.18}$$

yields

$$\sum_{r=0}^{\infty} q_r EI \phi_r'''' + \sum_{r=0}^{\infty} \ddot{q}_r \rho A \phi_r = f(x,t) \ . \tag{A.19}$$

Now each term is multiplied by $\phi_s(x)$ and the resultant expression is integrated with respect to x:

$$\sum_{r=0}^{\infty} q_r \int_0^{\ell} \phi_s EI \phi_r'''' dx + \sum_{r=0}^{\infty} \ddot{q}_r \int_0^{\ell} \rho A \phi_s \phi_r dx = \int_0^{\ell} \phi_s f(x,t) dx \ . \tag{A.20}$$

If the eigenpair ϕ_r, ω_r satisfies the undamped homogeneous differential Eq. (A.1), then

$$EI \phi_r'''' - \omega_r^2 \rho A \phi_r = 0$$

and

$$\int_0^\ell \phi_s EI\phi_r'''' dx = \omega_r^2 \int_0^\ell \phi_s \rho A \phi_r dx. \tag{A.21}$$

substituting Eq. (A.21) into Eq. (A.20) then yields

$$\sum_{r=0}^{\infty} q_r \omega_r^2 \int_0^\ell \rho A \phi_r \phi_s dx + \sum_{r=0}^{\infty} \ddot{q}_r \int_0^\ell \rho A \phi_r \phi_s dx = \int_0^\ell \phi_s f(x,t) dx. \tag{A.22}$$

Applying the orthogonality properties, this result reduces to the normal mode equations of motion,

$$M_r \ddot{q}_r + M_r \omega_r^2 q_r = Q_r(t), \quad r = 0, 1, 2, \ldots, \tag{A.23}$$

where $M_r = \int_0^\ell \rho A \phi_r^2(x) dx$ is the modal mass of the rth mode

and $Q_r = \int_0^\ell f(x,t) \phi_r(x) dx$ is the modal force of the rth mode.

Damping of the elastic modes can be taken into account by modifying Eq. (A.23) to the form

$$\ddot{q}_r + 2\zeta_r \omega_r \dot{q}_r + \omega_r^2 q_r = \frac{Q_{ra}(t)}{M_r} \tag{A.24}$$

where $Q_{ra}(t) = \int_0^\ell f_a(x,t) \phi_r(x) dx$ is the revised modal force, $f_a(x,t)$ is the prescribed excitation loading exclusive of damping forces, and ζ_r is the equivalent viscous damping ratio of the rth mode.

To obtain mobilities we will apply loads

$$f_a(x,t) = F(\omega) e^{i\omega t} \delta(x-\xi),$$

where $\delta(x-\xi)$ denotes the Diract delta function at location $x = \xi$.

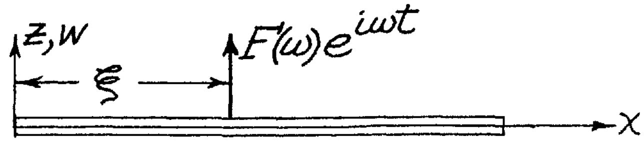

The pertinent response for each mode will be the steady-state sinusoidal generalized displacement

$$q_r(t) = X_r(\omega)\, e^{i\omega t} \tag{A.25}$$

where amplitude $X_r(\omega)$ is complex. We will examine this response mode by mode:

<u>r = 0</u>

$\omega_0 = 0$

$M_0 = \rho A \int_0^\ell \phi_0^2 dx = \rho A \ell = m$

$Q_{0a} = \int_0^\ell F(\omega) e^{i\omega t} \delta(x-\xi) \cdot 1\, dx = F(\omega) e^{i\omega t}$

$$\ddot{q}_0 + 2\zeta_0 \omega_0 \dot{q}_0 + \omega_0^2 q_0 = -\omega^2 X_0(\omega) e^{i\omega t}$$
$$= \frac{Q_{0a}(t)}{M_0} = \frac{F(\omega) e^{i\omega t}}{m}$$

$$\therefore\ X_0(\omega) = \frac{F(\omega)}{-\omega^2 m} \tag{A.26}$$

<u>r = 1</u>

$\omega_1 = 0$

$M_1 = \rho A \int_0^\ell \phi_1^2 dx = \frac{\rho A \ell^3}{12} = \frac{m\ell^2}{12}$

$Q_{1a} = \int_0^\ell F(\omega) e^{i\omega t} \delta(x-\xi)(x - \frac{\ell}{2}) dx = F(\omega) e^{i\omega t} (\xi - \frac{\ell}{2})$

$$\ddot{q}_1 + 2\zeta_1 \omega_1 \dot{q}_1 + \omega_1^2 q_1 = -\omega^2 X_1(\omega) e^{i\omega t}$$
$$= \frac{Q_{1a}(t)}{M_1} = \frac{F(\omega) e^{i\omega t} (\xi - \frac{\ell}{2})}{m\ell^2/12}$$

$$\therefore\ X_1(\omega) = \frac{F(\omega)(\xi - \frac{\ell}{2})}{-\omega^2 m \ell^2/12} \tag{A.27}$$

r = 2,3,...

$$M_r = \rho A \int_0^{\ell} \phi_r^2 dx = \rho A \ell = m$$

$$Q_{ra} = \int_0^{\ell} F(\omega) e^{i\omega t} \delta(x-\xi)\phi_r(x) dx = F(\omega) e^{i\omega t}\phi_r(\xi)$$

$$\ddot{q}_r + 2\zeta_r\omega_r\dot{q}_r + \omega_r^2 q_r = (-\omega^2 + i\omega 2\zeta_r\omega_r + \omega_r^2) X_r(\omega) e^{i\omega t}$$
$$= \frac{Q_{ra}(t)}{M_r} = \frac{F(\omega)\phi_r(\xi)e^{i\omega t}}{m}$$

$$\therefore X_r(\omega) = \frac{F(\omega)\phi_r(\xi)}{m(\omega_r^2 - \omega^2 + i2\zeta_r\omega_r\omega)} \tag{A.28}$$

As a consequence of Eqs. (A.17) and (A.25), it follows that

$$\dot{w}(\eta,t) = \sum_{r=0}^{\infty} \phi_r(\eta)\dot{q}_r(t) = \sum_{r=0}^{\infty} i\omega\phi_r(\eta) X_r(\omega) e^{i\omega t}$$
$$\triangleq \dot{W}(\omega) e^{i\omega t}. \tag{A.29}$$

The mobility is then the ratio of the complex amplitude of the transverse velocity at η to the amplitude of the transverse force at ξ:

$$\frac{\dot{W}(\omega)}{F(\omega)} = \sum_{r=0}^{\infty} i\omega\phi_r(\eta)\frac{X_r(\omega)}{F(\omega)} \quad . \tag{A.30}$$

Using Eqs. (A.26), (A.27) and (A.28), we obtain the resulting expression for translational mobility:

$$\frac{\dot{W}(\omega)}{F(\omega)} = \frac{1}{i\omega m} + \frac{(\eta-\frac{\ell}{2})(\xi-\frac{\ell}{2})}{i\omega m\ell^2/12}$$
$$+\frac{i\omega}{m}\sum_{r=2}^{\infty}\frac{\phi_r(\eta)\,\phi_r(\xi)}{\omega_r^2-\omega^2+i2\zeta_r\omega_r\omega} \quad . \tag{A.31}$$

In accordance with Eqs. (2.5), (2.9) and (2.11), the rotational mobilities are given by:

$$\frac{\dot{W}(\omega)}{M(\omega)} = \frac{\partial}{\partial\xi}\frac{\dot{W}(\omega)}{F(\omega)}$$
$$= \frac{\eta-\ell/2}{i\omega m\ell^2/12} + \frac{i\omega}{m}\sum_{r=2}^{\infty}\frac{\phi_r(\eta)\phi_r'(\xi)}{\omega_r^2-\omega^2+i2\zeta_r\omega_r\omega}$$

$$\frac{\dot{\Theta}(\omega)}{F(\omega)} = \frac{\partial}{\partial\eta}\frac{\dot{W}(\omega)}{F(\omega)} \tag{A.32}$$
$$= \frac{\xi-\ell/2}{i\omega m\ell^2/12} + \frac{i\omega}{m}\sum_{r=2}^{\infty}\frac{\phi_r'(\eta)\phi_r(\xi)}{\omega_r^2-\omega^2+i2\zeta_r\omega_r\omega}$$

$$\frac{\dot{\Theta}(\omega)}{M(\omega)} = \frac{\partial^2}{\partial\eta\partial\xi}\frac{\dot{W}(\omega)}{F(\omega)}$$
$$= \frac{1}{i\omega m\ell^2/12} + \frac{i\omega}{m}\sum_{r=2}^{\infty}\frac{\phi_r'(\eta)\phi_r'(\xi)}{\omega_r^2-\omega^2+i2\zeta_r\omega_r\omega} \quad .$$

The series terms in the above expressions are truncated to highest mode numbers r = N for computation, where N is determined such that $\omega_{MAX}/\omega_N < 0.5$. The latter condition, in turn, ensures that the exact mobilities are approximated by the truncated series results within much less than 0.5 dB deviation.

APPENDIX B

COMPUTER PROGRAM THEOR

```
C
C *************PROGRAM THEOR*************
C
C PROGRAM TO CALCULATE, STORE, & PLOT THEORETICAL TRANSLATIONAL AND ROTATIONAL
C    MOBILITIES (MAGNITUDE & PHASE)
      INTEGER*2 RUNID1(40), CASEID(40)
      INTEGER*2 XLA(40), XLP(40)
      DIMENSION OMEGR(25),ANUM1(25),ANUM2(25), ANUM3(25),  ANUM4(25)
      DIMENSION AMMOB(1,210), PHMOB(1,210), XS(4)
      COMPLEX ADEND, AMOB
      DOUBLE PRECISION Z,DPRL,ALPHA,PR,PRX,PRXI
      DOUBLE PRECISION PHX, PHXI, PHPRX, PHPRXI,DBCSH,DBSNH
C DEFINE DOUBLE PRECISION SINH & COSH ARITHMETIC STATEMENT FUNCTIONS
      DBCSH(Z)= (DEXP(Z)+DEXP(-Z))/2.
      DBSNH(Z)= (DEXP(Z)-DEXP(-Z))/2.
      DATA XS/ 0.,2000.,-400.,400./
      DEFINE FILE 10 (15,420,U,NRP)
C NFREQS= NO. OF FORCING FREQS. (INTEGER) FOR WHICH MOBILITIES WILL BE CALCU-
C    LATED, SPACED UNIFORMLY, UP TO FMAX (FLOATING)
C CAUTION-   CHECK DIMENSION STATEMENT FOR ARRAY SIZE
C BEAM PROPERTIES: E=E(N/M**2), AI= I (M**4), AM= TOTAL MASS (KG), AL= LENGTH (
C    M), ZETA= ASSUMED DAMPING RATIO
      READ (8,80) RUNID1
      READ (8,95) NCASES
      READ (8,130) NFREQS, FMAX
      READ (8,100) E,AI,AM,AL,ZETA
   80 FORMAT(40A2)
   95 FORMAT(I10)
  130 FORMAT (I10, F10.0)
  100 FORMAT (E10.1, E10.2, 3F10.3)
      WRITE (5,90) RUNID1
      WRITE (5,140) E,AI,AM,AL,ZETA
      WRITE (5,160) NFREQS,FMAX
   90 FORMAT (2H1 ,40A2)
  140 FORMAT(3HOE=,E10.3,4H  I=,E10.3,4H  M=,F5.2,4H  L=,F5.3,
     1 7H  ZETA=,F7.4)
  160 FORMAT(14HONO OF FREQS =,I4,12H  MAX FREQ =,F5.0///)
      DO 5000 NCASE= 1,NCASES
C X= LOCATION OF VELOCITY, XI= LOCATION OF FORCE OR MOMENT, KWF THRU KTHM ARE
C    CONTROLS OF WHICH TYPES OF MOBILITIES ARE GENERATED (1 FOR YES, 0 FOR NO),
C NPWF, ETC. ARE NOS. OF PLOTS OF EACH TYPE DESIRED: 0= NONE,1= MAGN. ONLY,
C    2= MAGN. & PHASE
C CAUTION- PLOT CONTROL DATA AND LABEL CARDS MUST BE PROVIDED CONSISTENT WITH
C    ABOVE INPUTS
C LSWF, ETC. ARE DISK LOCATIONS FOR STORAGE OF RESULTS- SUPPLY'0' WHEN MOBIL-
C    ITIES ARE NOT TO BE STORED
      READ (8,80) CASEID
      READ (8,110) X,XI,KWF,KWM,KTHF,KTHM
      READ (8,120) NPWF,NPWM,NPTHF,NPTHM
      READ (8,120) LSWF,LSWM,LSTHF,LSTHM
  110 FORMAT (2F10.2, 4I10)
  120 FORMAT(4I10)
      PIE= 3.141593
      RHOA= AM/AL
```

```
      PRAD= (E*AT/(RHOA*AL**4))**0.5
      RMAX= 0.5+(1./PIE)*(4.*PIE*FMAX/PRAD)**0.5
      NRMAX= RMAX+ 1.
      WRITE(5,90) CASEID
      WRITE (5,150) X,XI, KWF,KWM,KTHF,KTHM
      WRITE(5,155) NPWF,NPWM,NPTHF,NPTHM
      WRITE(5,156) LSWF,LSWM,LSTHF,LSTHM
  150 FORMAT(3H0X=,F6.3,5H  XI=,F6.3,6H  KWF=,I2,6H  KWM=,I2,7H  KTHF=,
     1 I2,7H  KTHM=,I2)
  155 FORMAT(6H0NPWF=,I1,8H,  NPWM=,I1,9H,  NPTHF=,I1,9H,  NPTHM=,I1)
  156 FORMAT(6H0LSWF=,I1,8H,  LSWM=,I1,9H,  LSTHF=,I1,9H,  LSTHM=,I1)
C CALCULATE MODAL PARAMETERS OF RECURRING USE
      WRITE (5,170)
  170 FORMAT(44H0  NATURAL FREQUENCIES OF VIBRATORY MODES,HZ/)
      DO 400 NR= 2, NRMAX
      IF (NR-3) 210,220,230
  210 PRL=4.730
      GO TO 240
  220 PRL= 7.853
      GO TO 240
  230 PRL= (2.0*FLOAT(NR)-1.0)*PIE/2.
  240 OMEGR(NR)= (PRL)**2*PRAD
      FREQNT= OMEGR(NR)/(2.*PIE)
      WRITE (5,300) FREQNT
  300 FORMAT (20X,F10.1)
      DPRL= DBLE(PRL)
      ALPHA= (DBSNH(DPRL)+DSIN(DPRL))/(DBCSH(DPRL)-DCOS(DPRL))
      PR= DBLE(PRL/AL)
      PRX= DBLE(PRL*X/AL)
      PRXI= DBLE(PRL*XI/AL)
      PHX=DBCSH(PRX)+DCOS(PRX)-ALPHA*(DBSNH(PRX)+DSIN(PRX))
      PHXI=DBCSH(PRXI)+DCOS(PRXI)-ALPHA*(DBSNH(PRXI)+DSIN(PRXI))
      PHPRX=PR*(DBSNH(PRX)-DSIN(PRX))-ALPHA*PR*(DBCSH(PRX)+DCOS(PRX))
      PHPRXI=PR*(DBSNH(PRXI)-DSIN(PRXI))-ALPHA*PR*
     1   (DBCSH(PRXI)+DCOS(PRXI))
      ANUM1(NR)= SNGL(PHX*PHXI)
      ANUM2(NR)= SNGL(PHX*PHPRXI)
      ANUM3(NR)= SNGL(PHPRX*PHXI)
      ANUM4(NR)= SNGL(PHPRX*PHPRXI)
  400 CONTINUE
C CALCULATE W/F MOBILITIES IF SPECIFIED IN INPUT DATA
 1000 IF (KWF-1) 2000,1010,1010
 1010 DO 1500 NPT= 1,NFREQS
      OMEGA= 2.*PIE*FMAX*FLOAT(NPT)/FLOAT(NFREQS)
      BNUM= (X-AL/2.)*(XI-AL/2.)
      BDEN= OMEGA*AM*(AL**2)/12.
      AMOB= CMPLX(1.0,0.0)/CMPLX(0.0,OMEGA*AM)+CMPLX(BNUM,0.0)/CMPLX
     1  (0.0,BDEN)
      DO 1400 NRR= 2, NRMAX
      RDEN= (OMEGR(NRR))**2 -OMEGA**2
      CDEN= 2.0*ZETA*OMEGR(NRR)*OMEGA
      ADEND= CMPLX(ANUM1(NRR),0.0)/CMPLX(RDEN,CDEN)
      CCOEF= OMEGA/AM
 1400 AMOB= AMOB+CMPLX(0.0,CCOEF)*ADEND
      AMMOB(1,NPT)= 20.*ALOG10(CABS(AMOB))
C MAGNITUDE IN DB RE 1 M/ NT SEC
```

```
      XX= REAL(AMOB)
      YY= AIMAG(AMOB)
      RPHMOB= ATAN2(YY,XX)
      PHMOB(1,NPT)= RPHMOB*180./PIE
 1500 CONTINUE
      IF (LSWF) 1520,1520,1510
 1510 WRITE(10'LSWF) (AMMOB(1,J),PHMOB(1,J),J=1,NFREQS)
      WRITE(5,1515)
 1515 FORMAT(' W/F MOBILITY FILED')
 1520 IF (NPWF-1) 2000,1530,1530
 1530 READ (8,1650) XLA
      CALL PICTR(AMMOB,1,XLA,XS,1,NFREQS,0,-1,4,1,FMAX,1)
      IF (NPWF-1) 2000,2000,1600
 1600 READ (8,1650) XLP
 1650 FORMAT (40A2)
      CALL PICTR(PHMOB,1,XLP,XS,1,NFREQS,0,-1,4,-2,FMAX,1)
C CALCULATE W/M MOBILITIES IF SPECIFIED IN INPUT DATA
 2000 IF (KWM-1) 3000,2010,2010
 2010 DO 2500 NPT= 1,NFREQS
      OMEGA= 2.*PIE*FMAX*FLOAT(NPT)/FLOAT(NFREQS)
      BNUM = X-AL/2.
      BDEN= OMEGA*AM*(AL**2)/12.
      AMOB= CMPLX(BNUM,0.0)/CMPLX(0.0,BDEN)
      DO 2400 NRR= 2,NRMAX
      RDEN= (OMEGR(NRR))**2 -OMEGA**2
      CDEN= 2.0*ZETA*OMEGR(NRR)*OMEGA
      ADEND= CMPLX(ANUM2(NRR),0.0)/CMPLX(RDEN,CDEN)
      CCOEF= OMEGA/AM
 2400 AMOB= AMOB+(CMPLX(0.0,CCOEF))*ADEND
      AMMOB(1,NPT)= 20.*ALOG10(CABS(AMOB))
C MAGNITUDE IN DB RE 1/ NT SEC
      XX= REAL(AMOB)
      YY= AIMAG(AMOB)
      RPHMOB= ATAN2(YY,XX)
      PHMOB(1,NPT)= RPHMOB*180./PIE
 2500 CONTINUE
      IF (LSWM) 2520,2520,2510
 2510 WRITE (10,LSWM)(AMMOB(1,J),PHMOB(1,J),J=1,NFREQS)
      WRITE (5,2515)
 2515 FORMAT (' W/M MOBILITY FILED')
 2520 IF (NPWM-1) 3000,2530,2530
 2530 READ (8,2650) XLA
      CALL PICTR(AMMOB,1,XLA,XS,1,NFREQS,0,-1,4,1,FMAX,1)
      IF (NPWM-1) 3000,3000,2600
 2600 READ (8,2650) XLP
 2650 FORMAT (40A2)
      CALL PICTR(PHMOB,1,XLP,XS,1,NFREQS,0,-1,4,-2,FMAX,1)
C CALCULATE THETA/F MOBILITIES IF SPECIFIED IN INPUT DATA
 3000 IF (KTHF-1) 4000,3010,3010
 3010 DO 3500 NPT= 1, NFREQS
      OMEGA= 2.*PIE*FMAX*FLOAT(NPT)/FLOAT(NFREQS)
      BNUM= XT-AL/2.
      BDEN= OMEGA*AM*(AL**2)/12.
      AMOB= CMPLX(BNUM,0.0)/CMPLX(0.0,BDEN)
      DO 3400 NRR= 2,NRMAX
      RDEN= (OMEGR(NRR))**2 -OMEGA**2
```

```
      CDEN= 2.0*ZETA*OMEGR(NRR)*OMEGA
      ADEND= CMPLX(ANUM3(NRR),0.0)/CMPLX(RDEN,CDEN)
      CCOEF= OMEGA/AM
 3400 AMOB= AMOB+(CMPLX(0.0,CCOEF))*ADEND
      AMMOB(1,NPT)= 20.*ALOG10(CABS(AMOB))
C MAGNITUDE IN DB RE 1 RAD/ NT SEC
      XY= REAL(AMOB)
      YY= AIMAG(AMOB)
      RPHMOB= ATAN2(YY,XY)
      PHMOB(1,NPT)= RPHMOB*180./PIE
 3500 CONTINUE
      IF (LSTHF) 3520,3520,3510
 3510 WRITE (10'LSTHF) (AMMOB(1,J),PHMOB(1,J),J=1,NFREQS)
      WRITE (5,3515)
 3515 FORMAT (' TH/F MOBILITY FILED')
 3520 IF (NPTHF-1) 4000,3530,3530
 3530 READ (8,3650) XLA
      CALL PICTR(AMMOB,1,XLA,XS,1,NFREQS,0,-1,4,1,FMAX,1)
      IF (NPTHF-1) 4000,4000,3600
 3600 READ (8,3650) XLP
 3650 FORMAT (40A2)
      CALL PICTR(PHMOB,1,XLP,XS,1,NFREQS,0,-1,4,-2,FMAX,1)
C CALCULATE THETA/M MOBILITIES IF SPECIFIED IN INPUT DATA
 4000 IF (KTHM-1) 5000,4010,4010
 4010 DO 4500 NPT= 1,NFREQS
      OMEGA= 2.*PIE*FMAX*FLOAT(NPT)/FLOAT(NFREQS)
      BDEN= OMEGA*AM*(AL**2)/12.
      AMOB= CMPLX(1.0,0.0)/CMPLX(0.0,BDEN)
      DO 4400 NRR= 2,NRMAX
      RDEN= (OMEGR(NRR))**2 -OMEGA**2
      CDEN= 2.0*ZETA*OMEGR(NRR)*OMEGA
      ADEND= CMPLX(ANUM4(NRR),0.0)/CMPLX(RDEN,CDEN)
      CCOEF= OMEGA/AM
 4400 AMOB= AMOB+CMPLX(0.0,CCOEF)*ADEND
      AMMOB(1,NPT)= 20.*ALOG10(CABS(AMOB))
C MAGNITUDE IN DB RE 1 RAD/ NT M SEC
      XY= REAL(AMOB)
      YY= AIMAG(AMOB)
      RPHMOB= ATAN2(YY,XY)
      PHMOB(1,NPT)= RPHMOB*180./PIE
 4500 CONTINUE
      IF (LSTHM) 4520,4520,4510
 4510 WRITE (10'LSTHM) (AMMOB(1,J),PHMOB(1,J),J=1,NFREQS)
      WRITE (5,4515)
 4515 FORMAT (' TH/M MOBILITY FILED')
 4520 IF (NPTHM-1) 5000,4530,4530
 4530 READ (8,4650) XLA
      CALL PICTR(AMMOB,1,XLA,XS,1,NFREQS,0,-1,4,1,FMAX,1)
      IF (NPTHM-1) 5000,5000,4600
 4600 READ (8,4650) XLP
 4650 FORMAT (40A2)
      CALL PICTR(PHMOB,1,XLP,XS,1,NFREQS,0,-1,4,-2,FMAX,1)
 5000 CONTINUE
      CALL EXIT
      END
```

APPENDIX C

COMPUTER PROGRAM TRANS

```
C
C*************PROGRAM TRANS*************
C
C PROGRAM TO CALCULATE, STORE, & PLOT TRANSLATIONAL MOBILITY FUNCTIONS FROM
C  COHER PROGRAM EXP'TAL SPECTRAL DATA-  ALSO PLOTS STORED THEOR. MOBILITIES
      INTEGER*2 IDTAPE(40),XLA(40),XLPH(40)
      DIMENSION ARRAY(7,210),AMSCL(4),PHSCL(4)
      DATA PHSCL/ 0.,2000.,-400.,400./
      DEFINE FILE 10(20,420,U,NRP)
      DEFINE FILE 11(15,420,U,NRQ)
C READ NO. OF TAPES TO BE PROCESSED IN THIS RUN
      READ(8,100) NTAPES
  100 FORMAT(I2)
      DO 1000 NT=1,NTAPES
C READ IN CONTROL DATA FOR EACH TAPE
C  IAMSCL=1 FOR AUTOSCALED MAGNITUDE PLOT; -2 FOR SCALING PER AMSCL DATA
C  LLAB=-4 FOR EXP'TAL DATA TO BE CONNECTED BY LINES; -4004 FOR DATA SYMBOLS;
C   THEOR. DATA CONNECTED BY LINES IN EITHER CASE
C  IAMCON=-10 TO PLOT EXP'TAL & THEOR. MAGNITUDES; -8 FOR EXP'TAL ONLY
C  IPHCON=-68 TO PLOT EXP'TAL & THEOR. PHASE; -64 FOR EXP'TAL ONLY
      READ (8,200)  IDTAPE,   LSM,NFREQS,NPLOTS,NLIST,NPR,LSTHEO,FMAX
      READ (8,205) (AMSCL(I),I=1,4),IAMSCL,LLAB,IAMCON,IPHCON
  200 FORMAT(40A2/6I10,F10.0)
  205 FORMAT (4F10.0,4I10)
C READ PLOT LABELS IF APPLICABLE
      IF (NPLOTS-1) 240,210,210
  210 READ (8,220) XLA
  220 FORMAT(40A2)
      IF (NPLOTS-1) 240,240,230
  230 READ (8,220) XLPH
C READ ONE TAPE'S DATA FROM CARDS
  240 READ(8,300)((ARRAY(I,J),I=1,4),J=1,NFREQS)
  300 FORMAT (F6.0,F6.1,6X,2F6.1)
      IF (NLIST) 400,400,350
C LIST INPUT DATA IF SPECIFIED (NLIST = 1)
  350 WRITE (5,360) ((ARRAY(I,J),I=1,4),J=1,NFREQS)
  360 FORMAT ('         FREQ           PSDF            CPSDAF           PHIAF'
     1//(7X,F5.0,3E15.4))
C REDUCE COHERENCE PROGRAM DATA
C  NOTE- NO IMPEDANCE HEAD MASS OR FLEXIBILITY CORRECTIONS INCLUDED
  400 DO 500 I=1,NFREQS
      W= 6.28318*ARRAY(1,I)
      ALM = 2.*(ARRAY(3,I)-ARRAY(2,I)) -20.*ALOG10(W)
      PHASE = ARRAY(4,I) - 90.
      ARRAY(4,I) = ALM
      IF (PHASE - 180.) 420,420,410
  410 PHASE = PHASE - 360.
  420 IF (PHASE + 180.) 430,440,440
  430 PHASE = PHASE + 360.
  440 ARRAY(7,I) = PHASE
      AMGN = 10.**(ALM/20.)
      PHASE = PHASE / 57.29578
      ARRAY(2,I) = AMGN * COS(PHASE)
      ARRAY(3,I) = AMGN * SIN (PHASE)
```

```
  500 CONTINUE
      IF (LSM) 565,565,550
C WRITE MOBILITY CO & QUAD COMPONENTS ONTO DISK IF LSM>0
  550 WRITE(10'LSM) ((ARRAY(I,J),I=2,3),J=1,NFREQS)
      WRITE (5,560)
  560 FORMAT ('EXPERIMENTAL MOBILITY FILED')
  565 IF (LSTHEO)  575,575,570
C READ THEORETICAL MOBILITY FROM DISK IF LSTHEO>0
  570 READ (11'LSTHEO)((ARRAY(I,J),I=2,3),J=1,NFREQS)
      WRITE (5,572)
  572 FORMAT ('THEORETICAL MOBILITY READ FROM FILE')
  575 WRITE(5,600) IDTAPE,LSM,NFREQS,NPLOTS,FMAX,LSTHEO
  600 FORMAT(21H1DATA IDENTIFICATION:,40A2//4X,'LSM=',I2,'  NFREQS=',
     1  I3,'  NPLOTS=',I1,'  FMAX=',F5.0,'   LSTHEO=',I2///)
      IF (NPR) 650,650,625
C PRINT OUTPUT DATA IF SPECIFIED (NPR=1)
  625 WRITE(5,640) ((ARRAY(I,J),I=1,5),J=1,NFREQS)
  640 FORMAT('       FREQ           CO           QUAD           MAGN
     1 PHASE'//(3X,F5.0,   3E15.4,,F10.2))
  650 IF (NPLOTS-1) 1000,700,700
C PLOT MOBILITY MAGNITUDE IF NPLOTS=1 OR 2
  700 CALL PICTR(ARRAY,7,XLA,AMSCL,IAMCON,NFREQS,0,-1,LLAB,IAMSCL,FMAX,
     1 1)
      IF (NPLOTS-1) 1000,1000,900
C PLOT MOBILITY PHASE IF NPLOTS= 2
  900 CALL PICTR(ARRAY,7,XLPH,PHSCL,IPHCON,NFREQS,0,-1,LLAB,-2,FMAX,1)
 1000 CONTINUE
      STOP
      END
```

APPENDIX D

COMPUTER PROGRAM ROTAT

```
C
C*************PROGRAM ROTAT************
C
C PROGRAM TO CALCULATE, STORE, & PLOT ROTATIONAL MOBILITIES FROM STORED TRANSLA-
C    TIONAL MOBILITIES USING BACKWARD DIFFERENCES
      INTEGER*2 RUNID(40), LAMAG(40),LAPH(40)
      DIMENSION SYMN(2,210),SYMN1(2,210),SYMN2(2,210)
      DIMENSION SYM1N(2,210),SYM1N1(2,210),SYM1N2(2,210)
      DIMENSION SYM2N(2,210),SYM2N1(2,210),SYM2N2(2,210)
      DIMENSION PHS(4), WFS(4), WMS(4), THFS(4), THMS(4)
      DATA PHS/0.,2000.,-400.,400./
      DEFINE FILE 10 (20,420,U,NRP)
      DEFINE FILE 11 (6,420,U,NRQ)
C READ RUN IDENTIFICATION DATA
      READ (8,90) RUNID
   90 FORMAT(40A2)
C READ MOTION & EXCITATION LOCATION NOS. AND WHICH TYPES OF MOBILITY ELEMENTS
C    ARE TO BE CREATED:
      READ(8,100) NX,NXI,KWFEX,KWMEX,KTHFEX,KTHMEX
  100 FORMAT(6I5)
C READ MEASUREMENT POINT NUMBERS M, M-1, M-2, AND DRIVING POINT NUMBERS N,
C    N-1, N-2; SUPPLY '0' WHERE NUMBER IS N/A:
      READ (8,100) M,M1,M2,N,N1,N2
C READ POINT SPACING VALUES (UNITS= M.), NO. OF FREQS., MAX. FREQ.:
C CAUTION: CHECK DIMENSION STATEMENTS FOR ARRAY SIZES VS. INPUT NO. OF FREQS.
      READ (8,225) DELTX,DELTXI,NFREQS,FMAX
  225 FORMAT(2F5.3,I5,F5.0)
C READ DISK LOCATION NUMBERS OF TRANSLAT. MOBILITY FILES TO BE READ-  SUPPLY
C    '0' WHERE NUMBER IS N/A:
      READ (8,250)LSMN,LSM1N,LSM2N,LSMN1,LSM1N1,LSM2N1,LSMN2,LSM1N2,
     1 LSM2N2
  250 FORMAT(9I5)
C READ DISK LOCATIONS FOR STORAGE OF RESULTS- SUPPLY '0' WHERE NUMBER IS N/A:
      READ (8,300) LSWFX,LSWMX,LSTHFX,LSTHMX
  300 FORMAT(4I5)
C READ NO. OF PLOTS OF EACH TYPE OF MOBILITY DESIRED: 0=NONE; 1= MAGN. ONLY;
C    2= MAGN. AND PHASE
      READ (8,300) NPWF,NPWM,NPTHF,NPTHM
C READ SCALE DATA FOR MAGNITUDE PLOTS
      READ (8,320) ( WFS(I), I=1,4)
      READ (8,320) ( WMS(I), I=1,4)
      READ (8,320) (THFS(I), I=1,4)
      READ (8,320) (THMS(I), I=1,4)
  320 FORMAT (4F10.0)
C PRINT OUT INPUT CONTROL DATA
      WRITE(5,325) RUNID
  325 FORMAT(1H1,40A2)
      WRITE(5,350)NX,NXI,KWFEX,KWMEX,KTHFEX,KTHMEX
      WRITE(5,400) M,M1,M2,N,N1,N2
      WRITE(5,425) DELTX,DELTXI,NFREQS,FMAX
      WRITE(5,450)LSMN,LSM1N,LSM2N,LSMN1,LSM1N1,LSM2N1,LSMN2,LSM1N2,
     1 LSM2N2
      WRITE(5,500) LSWFX,LSWMX,LSTHFX,LSTHMX
      WRITE(5,525) NPWF,NPWM,NPTHF,NPTHM
```

```
  350 FORMAT('0COMPUTE MOBILITIES FOR MOTION LOCATION' ,I2,'AND EXCITAT
     1 ION LOCATION' ,I2//'0    KWFEX=',I1,',    KWMEX=',I1,',    KTHFEX='
     2,I1,',    KTHMEX=',I1/)
  400 FORMAT('0    MEASUREMENT PTS.:  M IS ',I2,',    M1 IS ',I2,',    M2
     1IS ',I2/'    FORCING PTS.:  N IS ',I2,',    N1 IS ',I2,',    N2 IS '
     2,I2/)
  425 FORMAT('0    POINT SPACING VALUES:  DELTX=',F5.3,',    DELTXI =',
     1F5.3//'    NO. OF FREQS.=',I3,',    MAX. FREQ.=',F5.0/)
  450 FORMAT('0INPUT TRANSL. MOBILITY DISK STORAGE LOCATIONS:'/20X,'(M,N
     1) IS ',I2,',    (M,N-1) IS ',I2,',    (M,N-2) IS ',I2/20X,'(M-1,N) I
     2S ',I2,',    (M-1,N-1) IS ',I2,',    (M-1,N-2) IS ',I2/20X,'(M-2,N)
     3IS ',I2,',    (M-2,N-1) IS ',I2,',    (M-2,N-2) IS ',I2/)
  500 FORMAT('0OUTPUT MOBILITY DISK STORAGE LOCATIONS:'/'    W/F IS ',
     1I2,',    W/M IS ',I2,',    TH/F IS ',I2,',    TH/M IS ',I2/)
  525 FORMAT('0EXPERIMENTAL PLOTS TO BE MADE:  W/F:',I1,',  W/M:',I1,',
     1 TH/F:',I1,',    TH/M:',I1)
C READ TRANSL. MOBILITY DATA FROM DISK ONTO ARRAYS:
      IF (KTHMEX-1) 600,550,550
  550 READ (10'LSMN  ) ((SYMN  (I,J),I=1,2),J=1,NFREQS)
      READ (10'LSM1N ) ((SYM1N (I,J),I=1,2),J=1,NFREQS)
      READ (10'LSM2N ) ((SYM2N (I,J),I=1,2),J=1,NFREQS)
      READ (10'LSMN1 ) ((SYMN1 (I,J),I=1,2),J=1,NFREQS)
      READ (10'LSM1N1) ((SYM1N1(I,J),I=1,2),J=1,NFREQS)
      READ (10'LSM2N1) ((SYM2N1(I,J),I=1,2),J=1,NFREQS)
      READ (10'LSMN2 ) ((SYMN2 (I,J),I=1,2),J=1,NFREQS)
      READ (10'LSM1N2) ((SYM1N2(I,J),I=1,2),J=1,NFREQS)
      READ (10'LSM2N2) ((SYM2N2(I,J),I=1,2),J=1,NFREQS)
      GO TO 1000
  600 IF (KTHFEX-1) 700,650,650
  650 READ (10'LSMN  ) ((SYMN  (I,J),I=1,2),J=1,NFREQS)
      READ (10'LSM1N ) ((SYM1N (I,J),I=1,2),J=1,NFREQS)
      READ (10'LSM2N ) ((SYM2N (I,J),I=1,2),J=1,NFREQS)
  700 IF (KWMEX-1) 800,750,750
  750 READ (10'LSMN  ) ((SYMN  (I,J),I=1,2),J=1,NFREQS)
      READ (10'LSMN1 ) ((SYMN1 (I,J),I=1,2),J=1,NFREQS)
      READ (10'LSMN2 ) ((SYMN2 (I,J),I=1,2),J=1,NFREQS)
      GO TO 1000
  800 READ (10'LSMN  ) ((SYMN  (I,J),I=1,2),J=1,NFREQS)
C CALCULATE ROTATIONAL MOBILITIES:
 1000 DO 2000 NFR=1,NFREQS
      IF (KTHMEX-1) 1400,1100,1100
 1100 CO   =(9.*SYMN(1,NFR)-12.*SYMN1(1,NFR)+3.*SYMN2(1,NFR)-12.*SYM1N(1,
     1NFR)+16.*SYM1N1(1,NFR)-4.*SYM1N2(1,NFR)+3.*SYM2N(1,NFR)-4.*SYM2N1
     2(1,NFR)+SYM2N2(1,NFR))/(4.*DELTX*DELTXI)
      QUAD=(9.*SYMN(2,NFR)-12.*SYMN1(2,NFR)+3.*SYMN2(2,NFR)-12.*SYM1N(2,
     1NFR)+16.*SYM1N1(2,NFR)-4.*SYM1N2(2,NFR)+3.*SYM2N(2,NFR)-4.*SYM2N1
     2(2,NFR)+SYM2N2(2,NFR))/(4.*DELTX*DELTXI)
      SYM2N2(1,NFR)= CO
      SYM2N2(2,NFR)= QUAD
 1400 IF (KTHFEX-1) 1800,1500,1500
 1500 CO   = (3.*SYMN(1,NFR)-4.*SYM1N(1,NFR)+SYM2N(1,NFR))/(2.*DELTX)
      QUAD= (3.*SYMN(2,NFR)-4.*SYM1N(2,NFR)+SYM2N(2,NFR))/(2.*DELTX)
      SYM2N(1,NFR)= CO
      SYM2N(2,NFR)= QUAD
 1800 IF (KWMEX-1) 2000,1900,1900
 1900 CO   = (3.*SYMN(1,NFR)-4.*SYMN1(1,NFR)+SYMN2(1,NFR))/(2.*DELTXI)
```

```
      QUAD= (3.*SYMN(2,NFR)-4.*SYMN1(2,NFR)+SYMN2(2,NFR))/(2.*DELTXI)
      SYMN2(1,NFR)= CO
      SYMN2(2,NFR)= QUAD
 2000 CONTINUE
C WRITE THE RESULTANT MOBILITIES ONTO DISK:
      IF (LSWFX-1) 2200,2100,2100
 2100 WRITE(11'LSWFX ) ((SYMN  (I,J),I=1,2),J=1,NFREQS)
      WRITE(5,2150)
 2150 FORMAT('OW/F MOBILITY CO & QUAD FILED')
 2200 IF (LSWMX-1) 2400,2300,2300
 2300 WRITE(11'LSWMX ) ((SYMN2 (I,J),I=1,2),J=1,NFREQS)
      WRITE(5,2350)
 2350 FORMAT('OW/M MOBILITY CO & QUAD FILED')
 2400 IF (LSTHFX-1) 2600,2500,2500
 2500 WRITE(11'LSTHFX) ((SYM2N (I,J),I=1,2),J=1,NFREQS)
      WRITE(5,2550)
 2550 FORMAT('OTH/F MOBILITY CO & QUAD FILED')
 2600 IF (LSTHMX-1) 2800,2700,2700
 2700 WRITE(11'LSTHMX) ((SYM2N2(I,J),I=1,2),J=1,NFREQS)
      WRITE(5,2750)
 2750 FORMAT('OTH/M MOBILITY CO & QUAD FILED')
 2800 CONTINUE
C COMPUTE MAGNITUDE AND PHASE DATA, STORE IN SAME ARRAYS, AND PLOT:
 2900 IF (NPWF-1) 3100,3000,3000
 3000 DO 3050 NFR=1,NFREQS
      AMOB2=SYMN(1,NFR)**2 +SYMN(2,NFR)**2
      AMAGN= 10.*ALOG10(AMOB2+1.E-30)
      SYM1N(2,NFR)= ATAN2(SYMN(2,NFR),SYMN(1,NFR))*57.29578
 3050 SYMN(1,NFR)= AMAGN
      CALL MOVE (                 '                    FREQUENCY,  HZ
     *W/F MOBILITY MAGN., DB RE 1 M/ NT SEC    ',0,LAMAG,0,80)
      CALL MOVE (                 '                    FREQUENCY,  HZ
     *        W/F MOBILITY PHASE,  DEG.         ',0,LAPH,0,80)
      CALL PICTR(SYMN,1, LAMAG,WFS,-1,NFREQS,0,-1,-1004,-2,FMAX,1)
      IF (NPWF-1) 3100,3100,3060
 3060 CALL PICTR(SYM1N ,2,LAPH,PHS ,-2,NFREQS,0,-1,-2004,-2,FMAX,1)
 3100 IF (NPWM-1) 3300,3200,3200
 3200 DO 3250 NFR= 1,NFREQS
      AMOB2=SYMN2(1,NFR)**2 +SYMN2(2,NFR)**2
      AMAGN= 10.*ALOG10(AMOB2+1.E-30)
      SYMN2(2,NFR)= ATAN2(SYMN2(2,NFR),SYMN2(1,NFR))*57.29578
 3250 SYM2N1(1,NFR)= AMAGN
      CALL MOVE (                 '                    FREQUENCY,  HZ
     *W/M MOBILITY MAGN., DB RE 1/ NT SEC      ',0,LAMAG,0,80)
      CALL MOVE (                 '                    FREQUENCY,  HZ
     *        W/M MOBILITY PHASE,  DEG.         ',0,LAPH,0,80)
      CALL PICTR(SYM2N1,1,LAMAG,WMS,-1,NFREQS,0,-1,-1004,-2,FMAX,1)
      IF (NPWM-1) 3300,3300,3260
 3260 CALL PICTR(SYMN2,2,LAPH,PHS,-2,NFREQS,0,-1,-2004,-2,FMAX,1)
 3300 IF (NPTHF-1) 3500,3400,3400
 3400 DO 3450 NFR= 1,NFREQS
      AMOB2=SYM2N(1,NFR)**2 +SYM2N(2,NFR)**2
      AMAGN= 10.*ALOG10(AMOB2+1.E-30)
      SYMN1(2,NFR)= ATAN2(SYM2N(2,NFR),SYM2N(1,NFR))*57.29578
 3450 SYM2N(1,NFR)= AMAGN
      CALL MOVE (                 '                    FREQUENCY,  HZ
```

```
     *TH/F MOBILITY MAGN., DB RE 1/ NT SEC        ',0,LAMAG,0,80)
      CALL MOVE (                 '                 FREQUENCY,  HZ
     *        TH/F MOBILITY PHASE,  DEG.          ',0,LAPH,0,80)
      CALL PICTR(SYM2N,1,LAMAG,THFS,-1,NFREQS,0,-1,-1004,-2,FMAX,1)
      IF (NPTHF-1) 3500,3500,3460
 3460 CALL PICTR(SYMN1,2,LAPH,PHS,-2,NFREQS,0,-1,-2004,-2,FMAX,1)
 3500 IF (NPTHM-1) 3700,3600,3600
 3600 DO 3650 NFR= 1,NFREQS
      AMOB2=SYM2N2(1,NFR)**2 +SYM2N2(2,NFR)**2
      AMAGN= 10.*ALOG10(AMOB2+1.E-30)
      SYM2N2(2,NFR)= ATAN2(SYM2N2(2,NFR),SYM2N2(1,NFR))*57.29578
 3650 SYM1N2(1,NFR)= AMAGN
      CALL MOVE (                 '                 FREQUENCY,  HZ
     *TH/M MOBILITY MAGN., DB RE 1/ NT M SEC      ',0,LAMAG,0,80)
      CALL MOVE (                 '                 FREQUENCY,  HZ
     *        TH/M MOBILITY PHASE,  DEG.          ',0,LAPH,0,80)
      CALL PICTR(SYM1N2,1,LAMAG ,THMS,-1,NFREQS,0,-1,-1004,-2,FMAX,1)
      IF (NPTHM-1) 3700,3700,3660
 3660 CALL PICTR(SYM2N2,2,LAPH,PHS,-2,NFREQS,0,-1,-2004,-2,FMAX,1)
 3700 CALL EXIT
      END
```